Available online at www.sciencedirect.com

ScienceDirect

Geochimica et Cosmochimica Acta 220 (2018) 512–534

Geochimica et Cosmochimica Acta

www.elsevier.com/locate/gca

Mineralogy, early marine diagenesis, and the chemistry of shallow-water carbonate sediments

J.A. Higgins [a,*], C.L. Blättler [a], E.A. Lundstrom [a], D.P. Santiago-Ramos [a], A.A. Akhtar [a], A-S. Crüger Ahm [a], O. Bialik [a,b], C. Holmden [c], H. Bradbury [d], S.T. Murray [e], P.K. Swart [e]

[a] *Department of Geosciences, Princeton University, United states*
[b] *Leon H. Charney School of Marine Sciences, University of Haifa, Israel*
[c] *Department of Geological Sciences, University of Saskatchewan, Canada*
[d] *Department of Earth Sciences, Cambridge University, United Kingdom*
[e] *Rosenstiel School of Marine at Atmospheric Science, University of Miami, United states*

Received 15 March 2017; accepted in revised form 26 September 2017

Abstract

Shallow-water carbonate sediments constitute the bulk of sedimentary carbonates in the geologic record and are widely used archives of Earth's chemical and climatic history. One of the main limitations in interpreting the geochemistry of ancient carbonate sediments is the potential for post-depositional diagenetic alteration. In this study, we use paired measurements of calcium ($^{44}Ca/^{40}Ca$ or $\delta^{44}Ca$) and magnesium ($^{26}Mg/^{24}Mg$ or $\delta^{26}Mg$) isotope ratios in sedimentary carbonates and associated pore-fluids as a tool to understand the mineralogical and diagenetic history of Neogene shallow-water carbonate sediments from the Bahamas and southwest Australia. We find that the Ca and Mg isotopic composition of bulk carbonate sediments at these sites exhibits systematic stratigraphic variability that is related to both mineralogy and early marine diagenesis. The observed variability in bulk sediment Ca isotopes is best explained by changes in the extent and style of early marine diagenesis from one where the composition of the diagenetic carbonate mineral is determined by the chemistry of the fluid (fluid-buffered) to one where the composition of the diagenetic carbonate mineral is determined by the chemistry of the precursor sediment (sediment-buffered). Our results indicate that this process, together with variations in carbonate mineralogy (aragonite, calcite, and dolomite), plays a fundamental and underappreciated role in determining the regional and global stratigraphic expressions of geochemical tracers ($\delta^{13}C$, $\delta^{18}O$, major, minor, and trace elements) in shallow-water carbonate sediments in the geologic record. Our results also provide evidence that a large shallow-water carbonate sink that is enriched in ^{44}Ca can explain the mismatch between the $\delta^{44/40}Ca$ value of rivers and deep-sea carbonate sediments and call into question the hypothesis that the $\delta^{44/40}Ca$ value of seawater depends on the mineralogy of primary carbonate precipitations (e.g. 'aragonite seas' and 'calcite seas'). Finally, our results for sedimentary dolomites suggest that paired measurements of Ca and Mg isotopes may provide a unique geochemical fingerprint of mass transfer during dolomitization to better understand the paleo-environmental information preserved in these enigmatic but widespread carbonate minerals.

Keywords: Carbonate geochemistry; Isotopes; Carbon; Calcium; Magnesium

1. INTRODUCTION

The chemistry of shallow water marine carbonate sediments has been used to reconstruct the temperature

* Corresponding author.
E-mail addresses: jahiggin@princeton.edu, jahiggins@post.harvard.edu (J.A. Higgins).

https://doi.org/10.1016/j.gca.2017.09.046
0016-7037/

and isotopic composition of seawater as well as the global carbon and oxygen cycles over >3 billion years of Earth history (Veizer and Hoefs, 1976; Veizer et al., 1999). The underlying assumption in these studies is that the chemical composition of the sediment accurately preserves a record of ancient open-ocean seawater (Holmden et al., 1998; Immenhauser et al., 2003; Swart, 2008). One of the principal ways in which this assumption is violated is through diagenesis - the chemical changes that occur during the transformation of sediment into rock. Diagenetic alteration of carbonate sediments can occur in association with either meteoric or marine fluids (Ginsburg, 1957; Berner, 1966; Sass and Katz, 1982; Richter and DePaolo, 1987; Budd, 1997; Melim et al., 2004; Swart, 2015), is observed at length scales from microns (Kozdon et al., 2011) to stratigraphic units (Swart and Eberli, 2005), and may take the form of recrystallization (no change in mineralogy) or neomorphism (change in mineralogy). In some cases diagenetic alteration is regarded as the dominant source of variability in the geologic record (i.e. $\delta^{18}O$; (Muehlenbachs and Clayton, 1976)) whereas in other cases (i.e. $\delta^{13}C$) the effects of diagenesis are generally thought to be small though not insignificant (Banner and Hanson, 1990; Marshall, 1992). The effects of diagenesis, in particular *early marine diagenesis*, on many shallow-water carbonate-bound geochemical proxies (e.g. $\delta^{34}S$ values of carbonate-associated sulfate (CAS), $\delta^{44}Ca$, $\delta^{26}Mg$, $\delta^{7}Li$, $\delta^{11}B$, $\delta^{98/95}Mo$, $\delta^{238/235}U$ values, and I/Ca ratios) are either unknown or limited to a handful of studies (Fantle and DePaolo, 2007; Jacobson and Holmden, 2008; Higgins and Schrag, 2012; Romaniello et al., 2013; Fantle and Higgins, 2014; Rennie and Turchyn, 2014; Edgar et al., 2015; Geske et al., 2015b; Riechelmann et al., 2016).

Recent studies by Blättler et al. (2015) and Fantle and Higgins (2014) have shown both large variability and co-variation between the stable isotope ratios of magnesium ($^{26}Mg/^{24}Mg$) and calcium ($^{44}Ca/^{40}Ca$) in authigenic and diagenetic carbonates from the Monterey Formation (Miocene) in offshore southern California and the Marion Plateau off of northeast Australia (Ocean Drilling Program (ODP) Site 1196). In both cases the variability and co-variation are driven primarily by the extent to which diagenesis/authigenesis occurred in fluid-buffered or sediment-buffered conditions. Additional studies on Ca and Mg isotope fractionation in carbonates have shown that these systems depend on mineralogy – aragonite is depleted in ^{44}Ca and enriched in ^{26}Mg compared to calcite (Gussone et al., 2005) - as well as the rate of mineral precipitation and solution chemistry (Fantle and DePaolo, 2007; Tang et al., 2008; DePaolo, 2011; Nielsen et al., 2013). Importantly, the observed variability in the Ca and Mg isotopic composition of bulk carbonate sediments associated with changes in mineralogy and early diagenesis is large compared to other potential sources (e.g. changes in seawater $\delta^{26}Mg$ and $\delta^{44}Ca$ values (Griffith et al., 2008; Higgins and Schrag, 2015; Gothmann et al., 2016)), suggesting that these measurements can provide novel insights into both the primary mineralogy and early diagenetic history of carbonate-bound geochemical proxies.

Here we present a large data set ($N = 676$) of $\delta^{44}Ca$ and $\delta^{26}Mg$ values in Neogene carbonate sediments and associated pore-fluids from the Bahamas and the Eucla Shelf. The ten studied sites encompass a wide range of depositional, mineralogical, and diagenetic environments and were selected to explore whether these differences are associated with variations in sedimentary carbonate $\delta^{44}Ca$ and $\delta^{26}Mg$ values. At all studied sites we observe coherent stratigraphic variability in carbonate Ca and Mg isotopes that can be attributed largely to the effects of mineralogy and diagenesis under both fluid-dominated and rock-dominated conditions. The magnitude of the stratigraphic variability in Ca isotopes is large - >1‰ - and co-varies with bulk sediment geochemistry (Sr/Ca), $\delta^{13}C$, and $\delta^{18}O$ values. We interpret this variability as a consequence of changes in primary carbonate mineralogy and the extent to which the original carbonate sediment has been neomorphosed and/or recrystallized under fluid-buffered or sediment-buffered conditions. Measured pore-fluid profiles of $\delta^{44}Ca$ and $\delta^{26}Mg$ values support this interpretation and indicate that carbonate diagenesis under both fluid-buffered and sediment-buffered conditions is ongoing on the western flank of the GBB. This work demonstrates the importance of mineralogy and early diagenesis in shaping the chemistry of shallow-water carbonate sediments and highlights the utility of using paired measurements of Ca and Mg isotopes to identify and characterize these effects.

2. BACKGROUND/SITE DESCRIPTION

A total of ten sites were selected to explore the effects of both mineralogy and early diagenesis on the $\delta^{44}Ca$ and $\delta^{26}Mg$ values of shallow marine carbonate sediments in a geological (stratigraphic) context. Nine of the studied sites are from carbonate platform and slope environments in the Bahamas – five sites from a transect across the western flank of the Great Bahama Bank (GBB; (Eberli et al., 1997a)) and four sites from a transect across the Little Bahama Bank (LBB; (Vahrenkamp et al., 1991a)). The tenth site is ODP Site 1131, a Pliocene-Pleistocene succession of cool-water carbonates in the Great Australian Bight (Fig. 1).

2.1. The Bahamas

Western flank of the Great Bahama Bank (ODP Sites 1007, 1005, 1003, Clino, and Unda): The western flank of the Great Bahama Bank (GBB) is a modern example of a low-angle, prograding carbonate platform under the influence of changes in sea-level associated with Neogene glacial cycles (Eberli and Ginsburg, 1987; Eberli et al., 1997b; Ginsburg, 2001). The sediment produced on the Bahamas platform is largely composed of aragonite with minor amounts of high-Mg calcite (Swart et al., 2009). This bank-top sediment is either deposited on the shelf or exported to the slope where it mixes with variable amounts of carbonate sediment sourced from pelagic environments (Eberli et al., 1997a; Swart and Eberli, 2005). Studied sites from the Western flank of the GBB form a 25-km transect

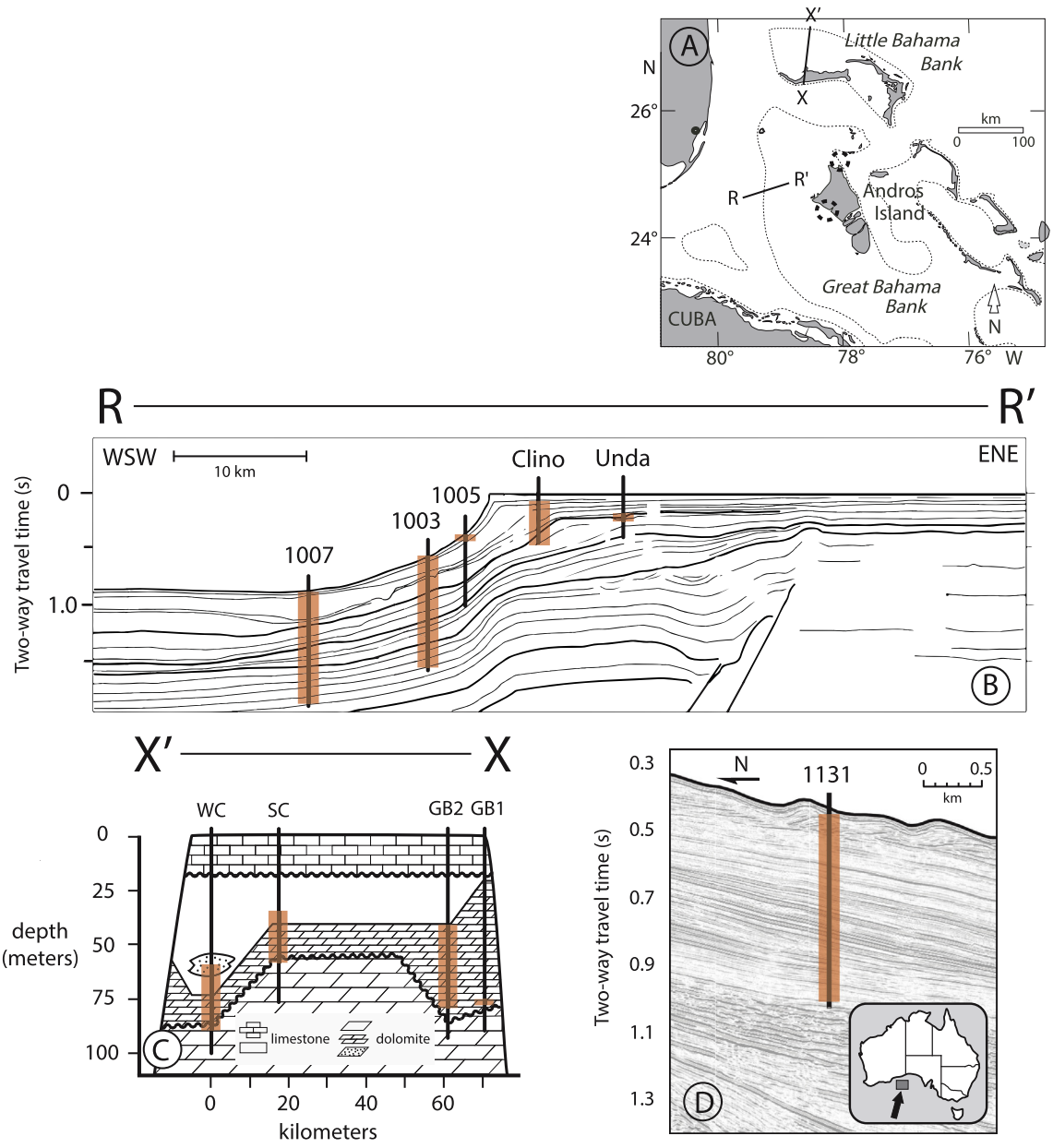

Fig. 1. Maps of sites used in this study. (A) Transects and study sites from the Bahamas. Lines R-R′ and X-X′ denote transects; dashed circles denote sample areas. (B) Transect along the western flank of the Great Bahama Bank. Shaded intervals denote depths were samples were taken. (C) Transect from the Little Bahama Bank. Shaded intervals denote depths where samples were taken. Different limestone/dolomite lithologies are indicated. (D) Site 1131 from the Eucla shelf in southwest Australia. Shaded interval denotes depths where samples were taken.

from depths of ~10 m below sea level (mbsl) in the platform interior (Unda) and margin (Clino), to >600 mbsl on the slope (Site 1007).

Detailed descriptions of the geochemistry, sedimentology and stratigraphy of each site from the GBB transect have been published elsewhere (Eberli et al., 1997a; Ginsburg, 2001) and are only briefly reviewed here. Unda sits at the NE end of the transect and consists of three successions of shallow-water platform and reefal deposits that alternate with intervals of deeper skeletal and peloidal platform margin deposits (Kenter et al., 2001). Subaerial exposure surfaces and intervals of pervasive dolomitization indicate that the sediments at Unda have seen a wide range of diagenetic conditions. Our samples are restricted to the dolomitized interval between 250 and 350 m below the seafloor (mbsf). Clino is located at the modern platform margin and is composed of three major lithologic units: an upper succession of shallow-water platform and reefal deposits (20–200 mbsf), a middle interval composed of fine-grained nonskeletal sediment with thin interbeds of coarse-grained skeletal material (200–370 mbsf), and a lower deeper unit consisting of mixtures of fine-grained skeletal and non-skeletal sediment with thin layers of coarser skeletal material (370–680 mbsf; (Kenter et al., 2001)).

Between 200 and 680 m, nearly 80% of the sediment in Clino consists of monotonous intervals of skeletal and peloidal sand and silt-sized grains. The remaining 20% of the sediment are intervals of coarse-grained skeletal packstones to grainstones; two of these intervals, marine hardgrounds at 367 and 536 m, represent prolonged periods of erosion and non-deposition on the slope. The mineralogy of carbonate sediments at Clino varies widely with depth (Fig. 2); between 34 and 150 m it consists almost entirely of low-Mg calcite, whereas between 150 and 367 m aragonite is abundant (up to 65 wt%). Below 367 mbsf dolomite makes up a common but minor fraction of the sediment with prominent peaks at 367 and 536 mbsf. In an effort to isolate the effects of dolomitization on sediment $\delta^{44}Ca$ and $\delta^{26}Mg$ values we measured a series of successive leach experiments (Swart and Melim, 2000) on two of the more heavily dolomitized intervals at Clino (366–378 mbsf and 494–646 mbsf). Each sample was leached once or twice, resulting in a total of two or three samples at each depth.

Ocean Drilling Program Sites 1005, 1003 and 1007 were drilled on the prograding western margin of the Great Bahama Bank on the middle slope (350 and 480 mbsl) and the toe of slope (650 mbsl), respectively (Fig. 1). Carbonate sedimentation at these sites consists almost entirely of a mixture of material sourced from the platform top (aragonite) with smaller contributions from pelagic sources (low-Mg calcite; (Eberli et al., 1997b)). The sedimentology of the sites is similar and units are generally characterized by mudstones and wackestones coarsening upwards to packstones, grainstones, and floatsones. Both sites are characterized by systematic changes in sediment mineralogy (as determined by XRD; (Eberli et al., 1997b; Melim et al., 2001)) and increasing lithification with depth. Aragonite is abundant in the upper 150–200 m of the sediment column but largely replaced by low-Mg calcite and minor amounts of dolomite (Fig. 2) at greater depths. To complement the measurements of bulk sediment $\delta^{44}Ca$ and $\delta^{26}Mg$ values we also measured $\delta^{44}Ca$ and $\delta^{26}Mg$ values in samples of sedimentary pore-fluids from Site 1003 and 1007 (Kramer et al., 2000). These measurements can provide constraints on rates of recrystallization/neomorphism/dolomitization and Ca and Mg isotopic fractionation associated with these diagenetic reactions (Fantle and DePaolo, 2007; Higgins and Schrag, 2010, 2012; Turchyn and DePaolo, 2011).

Little Bahama Bank (WC1, SC1, GB2, and GB1): The Little Bahama Bank (LBB) is the northernmost carbonate platform of the Bahamian Archipelago and hosts an extensive dolomite body in Neogene sediments at shallow depths (20–100 mbsf; Fig. 2). Previous studies on the petrography and geochemistry of these dolomites (Vahrenkamp et al., 1988, 1991a) indicate that the dolomitization occurred early after sediment deposition by a fluid that was essentially unaltered seawater. Depositional textures of the original (non-dolomitized) carbonate sediments range from wackestones to grainstones deposited in outer-reef to inner-platform environments. Biogenic carbonates commonly observed include corals, foraminifera, echinoderms, red algae, rhodoliths, and molluscs. Dolomitization of the sediment is generally complete and textures range from fabric-preserving to fabric-destructive. Studied samples are all dolomites from four wells drilled along a N-S transect of the LBB (Murray and Swart, 2017).

2.2. Southwest Australia

ODP Site 1131: Ocean Drilling Program Site 1131 is located on the upper slope (332.4 mbsl) adjacent to the Eucla Shelf, a mid-latitude cool-water carbonate deposit in the western Great Australian Bight (Feary et al., 2000). The site captures a set of rapidly accumulating (~25 cm/kyr), prograding clinoforms of Quaternary age. Sediments are predominately bioclastic packstones interrupted by occasional units of wackestone, grainstone and floatstone. Biogenic components include bryozoans (esp. 0–30 mbsf), foraminifera, echinoid spines, and nannofossils (Feary et al., 2000). In contrast to the Bahamas where surface sediments are dominated by aragonite, the mineralogy of the carbonate sediments at Site 1131 includes up to 60 wt% high-Mg calcite near the surface that declines to ~0 wt% by 70 m depth (Fig. 2). The decline in high-Mg calcite is mirrored by an increase in low-Mg calcite and minor amounts of dolomite. Aragonite is a minor (~10 wt%) constituent throughout the core (Swart et al., 2000).

3. ANALYTICAL METHODS

3.1. Sample preparation and ion chromatography

Samples for this study were analyzed in three different laboratories (Princeton University $N = 646$, University of Saskatchewan $N = 19$, and the University of Cambridge $N = 11$). At Princeton, samples for Ca and Mg isotope analyses were processed using an automated high-pressure ion chromatography (IC) system (Dionex ICS-5000+) following previously published methods (Fantle and Tipper, 2014; Blättler et al., 2015; Husson et al., 2015; Gothmann et al., 2016). At the University of Saskatchewan, carbonate samples were dissolved in 1.0 N HCl to make a stock solution. 50 μg of Ca was aliquoted from the stock solution and mixed with an isotopically enriched ^{43}Ca-^{42}Ca double-tracer to bring the mixed $^{40}Ca/^{42}Ca$ ratio to ~7.0 (Holmden, 2005). The sample-tracer mixtures were dried down to ensure spike-sample equilibration, and subsequently passed through traditional gravity-flow columns containing MP50-cation exchange resin to purify Ca from matrix elements. At Cambridge, sample aliquots containing 6 μg of calcium were combined with a ^{42}Ca-^{48}Ca double–spike at a ratio of 10:1 (sample-to-spike) in acid-cleaned Teflon vials. The 48:42 ratio of the double–spike is 1:1, similar to the optimum ratio of 3:2 for a ^{42}Ca-^{48}Ca double–spike (Rudge et al., 2009). Solid samples were dissolved in dilute ultra-pure acetic acid for 1 h, before being converted to nitrates and then combined with the double spike. The samples were then dried and re-dissolved in 0.5% nitric acid and calcium was separated using a Dionex ICS-5000^{+} IC system coupled with a Dionex AS-AP fraction collector. The method is similar to the published work of Schmitt et al. (2009). The procedural blank as determined by ICP-OES is 96ng of calcium, representing ~2% of the collected calcium.

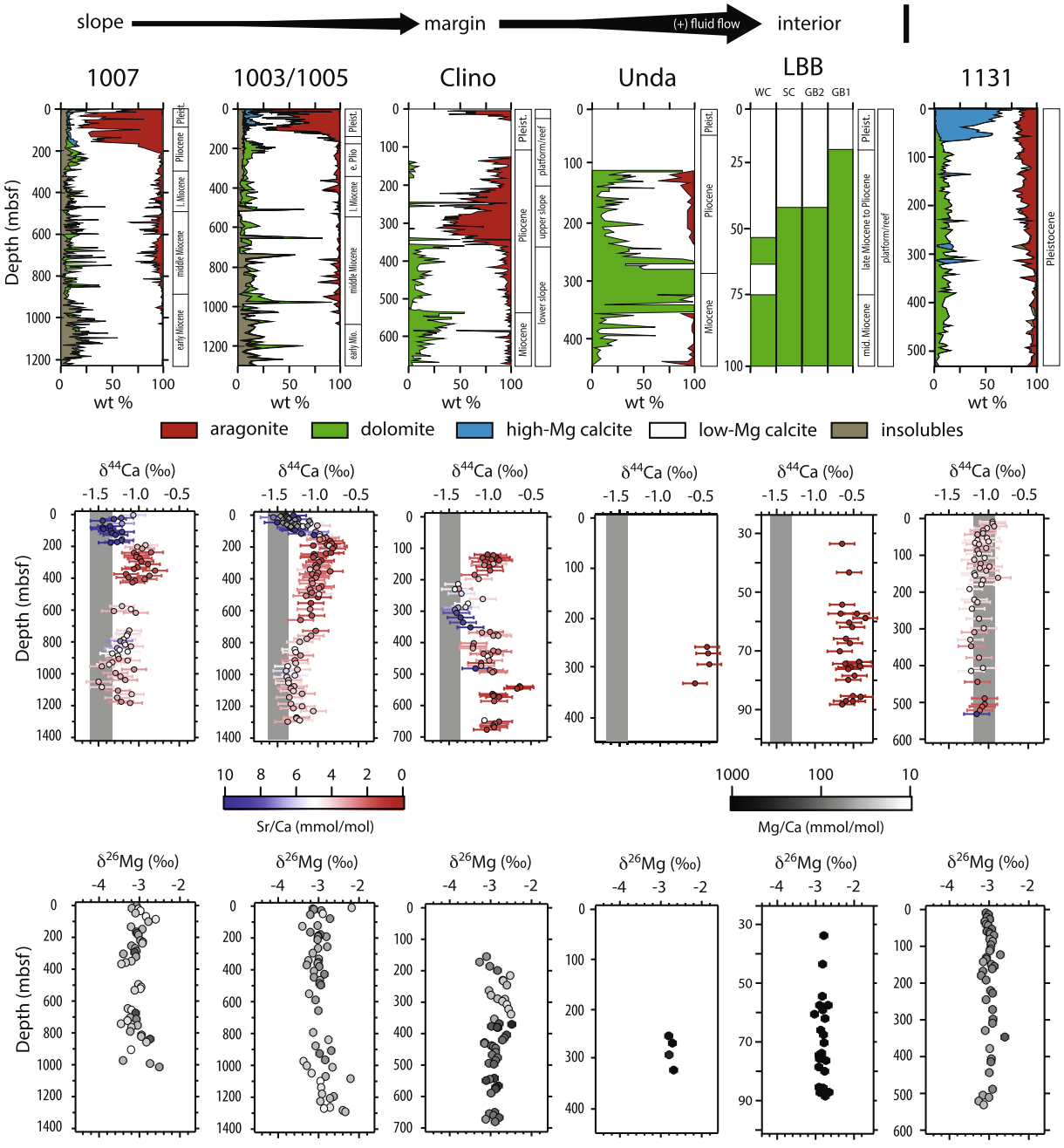

Fig. 2. Depth profiles of bulk sediment mineralogy (TOP), $\delta^{44}Ca$ values (MIDDLE) and $\delta^{26}Mg$ values (BOTTOM) for all studied sites. **TOP:** Aragonite is abundant in the upper ~200 m at Sites 1007 and 1003/1005 whereas peak aragonite abundance occurs at ~300 m at Clino. Aragonite is absent from studied samples from Unda and the LBB and is a minor component at Site 1131, where the dominant metastable carbonate is high-Mg calcite. Dolomite abundance increases from slope to platform margin and interior, a trend we interpret as reflecting the increasing importance of sedimentary fluid flow (which supplies Mg for dolomitization) in platform interiors. **MIDDLE:** Measured $\delta^{44}Ca$ values are colored based on bulk sediment Sr/Ca ratio. Grey symbols are samples from Site 1005 analyzed at the University of Saskatchewan. All other samples were analyzed at Princeton. High Sr/Ca ratios are generally associated with low $\delta^{44}Ca$ values. Shaded regions indicate range of $\delta^{44}Ca$ values for measured bank-top sediment (Table S1) and dotted lines at Clino denote prominent marine hardgrounds. For Site 1131, the shaded region is the same width as for the Bahamas sites, but is centered on the average $\delta^{44}Ca$ value for Site 1131. **BOTTOM:** Measured $\delta^{26}Mg$ values are colored based on bulk sediment Mg/Ca ratio. (For interpretation of the references to color in this figure legend, the reader is referred to the web version of this article.)

3.2. Dolomite Leachates

Dolomite in samples of mixed mineralogy were purified using the method outlined by Swart and Melim (Swart and Melim, 2000). In this method the sample is ground to less than 50 μm in size and treated with buffered acetic acid. After 60 min the reaction is quenched and the residual material subjected to X-ray diffraction to assess the effectiveness of the procedure. If the samples still contains non-dolomitic carbonate, the procedure is repeated. In this manner a series of leachates with varying amounts of dolomite is produced.

3.3. Mass spectrometry

At Princeton dissolved samples were analyzed for $\delta^{44}Ca$ and $\delta^{26}Mg$ values on a Thermo Scientific Neptune Plus multi-collector inductively-coupled plasma mass spectrometer (MC-ICP-MS; (Blättler and Higgins, 2014; Fantle and Higgins, 2014; Blättler et al., 2015; Husson et al., 2015; Gothmann et al., 2016). Minimum sample sizes are 4–5 μg for Ca and 0.5–1 μg for Mg for a single isotopic analysis (column chromatography and mass spectrometry). Measurements are carried out at low resolution for Mg and medium resolution for Ca to avoid $ArHH^+$ interferences. All data are reported in delta notation relative to a known standard for Ca isotopes and measured $\delta^{44/42}Ca$ values are converted to $\delta^{44/40}Ca$ values assuming mass-dependent fractionation with a slope of 2.05 and no excess radiogenic ^{40}Ca (Fantle and Tipper, 2014). Although almost all of the Sr^{2+} is separated from Ca during ion chromatography, we correct for occasional small Sr^{2+} isobaric interferences in the Ca measurements using measurements at $m/z = 43.5$ (doubly-charged $^{87}Sr^{2+}$). All Ca and Mg isotope values are plotted in 3-isotope space ($\delta^{26/24}Mg$ vs. $\delta^{25/24}Mg$ and $\delta^{44/42}Ca$ vs. $\delta^{43/42}Ca$) to verify that Mg and Ca isotope variability falls along the expected mass-dependent line.

Long-term external reproducibility for each isotopic system is determined based on the difference between two known standards taken through the full chemical procedure (column chromatography and mass spectrometry) with each batch of samples. For Ca isotopes we report external reproducibility using the measured value of SRM915b relative to modern seawater, both of which are processed and analyzed alongside a set of 20–30 samples on the same IC run. Our measured $\delta^{44/40}Ca$ value for SRM915b relative to modern seawater is -1.18 ± 0.16‰ (2σ; $N = 125$), indistinguishable from published values determined by both MC-ICP-MS and TIMS (Fantle and Tipper, 2014). All Ca isotope samples are reported relative to modern seawater ($\delta^{44}Ca_{seawater} = 0$‰). $\delta^{44}Ca_{seawater} = +1.92$‰ on the SRM915a scale and +0.98‰ on the bulk silicate Earth (BSE) scale (Fantle and Tipper, 2014). For Mg, the long-term external reproducibility of our measurements is estimated by comparing the Mg standard Cambridge-1 and modern seawater against Dead Sea Magnesium (DSM-3). Our measured $\delta^{26}Mg$ values for Cambridge-1 and seawater are -2.56 ± 0.09‰ (2σ, $N = 76$) and -0.83 ± 0.08‰ (2σ; $N = 99$), respectively, both indistinguishable from published values (Young and Galy, 2004). Reported errors for each sample depend on the number of times the sample has been separated and analyzed. For a single separation and analysis, we report the long-term external reproducibility of SRM915b or Cambridge-1 ($2\sigma = \pm 0.16$‰, and ± 0.09‰, respectively). For multiple chromatographic separations and analysis ($N > 1$) we also report the standard error of the mean (SE).

At the University of Saskatchewan, ~10–20 μg of Ca was loaded onto outgassed Ta filaments with phosphoric acid. The measurements were made in a dynamic peak hopping routine. Collector drift was monitored and corrected with standards that were run at the same time as the samples (Belanger and Holmden, 2010; Lehn et al., 2013). The estimated external reproducibility based on repeated measurements of samples and standards using the spike composition and measurement routines documented in Belanger and Holmden (2010) is ±0.07‰. All Ca isotope analyses are reported on the seawater scale. The $\delta^{44/40}Ca$ values for SRM 915a and 915b measured over the course of this study is –1.86‰ and –1.13‰.

At Cambridge the calcium pore fluid samples were run on a Thermo Scientific Triton Plus MC-TIMS. Purified calcium from each sample is in 1 μl of 2 M nitric-acid and 4 μg of calcium is loaded on an outgassed 0.7 mm Rhenium filament with 0.5 μl of 10% trace metal purity Phosphoric acid as an activator. The samples are run using a double filament method, with the ionisation filament being heated to 1400° (as measured on a pyrometer), and the evaporation filament is heated manually until a stable signal between 5 and 10 V of ^{40}Ca on a 10^{11} Ω resistor is reached. The method consists of a dynamic collection routine (40–44 and 42–48) with an integration time of 8.389 s. 10 blocks of 20 cycles are collected, with peak centring and baseline being run at the start of the run, and lens focusing occurring every 2nd block. Total run-time not including heating is 1.5 h. Five samples of SRM915b were run within each turret of 21 samples giving an average value of -1.14 ± 0.11‰ (2σ; $N = 10$) relative to modern seawater.

3.4. Major/minor element analyses

Aliquots of dissolved powders analyzed for Ca and Mg isotopes were also measured for Mg/Ca, Sr/Ca, Mn/Ca and U/Ca ratios on Thermo Finnigan Element-2 inductively coupled plasma mass spectrometer (ICP-MS) at Princeton University. The metal to calcium (Me/Ca) ratios of samples were determined using a set of matrix-matched in-house standards spanning the sample range (Rosenthal et al., 1999). The external reproducibility of the Me/Ca ratios are estimated at ±5–7% (2σ) from replicate measurements of SRM88b, a dolomitic limestone.

3.5. Other geochemical and mineralogical data

There is a large existing database of pore-fluid chemistry and sediment mineralogy, $\delta^{13}C$ (‰; VPDB scale), $\delta^{18}O$ (‰; VPDB scale), and $^{87}Sr/^{86}Sr$ values from previous studies on the sites from the Bahamas (Eberli et al., 1997b; Kramer et al., 2000; Swart, 2000, 2008) and the Eucla Shelf (Feary et al., 2000). Pore-fluid samples were taken

shipboard on 5- to 15- cm-long whole-round sections with a titanium squeezer, modified after the standard ODP stainless steel squeezer of Manheim and Sayles and Manheim (1975). All interstitial water samples were double-filtered and collected into acid-washed (10% HCl) 50-mL plastic syringes through 0.45 μm and 0.22 μm Gelman polysulfone disposable filters. For bulk sediment samples, when possible we have measured the same samples as those analyzed in previous studies, though in many cases our samples come from separate, but nearby (within a few meters) sections of the core. For the purpose of plotting pairs of geochemical data (i.e. $\delta^{13}C$ vs. $\delta^{44}Ca$) these nearby samples are regarded as a pair (Table S1). Different choices on how to pair samples or interpolate the geochemical data do not significantly affect the results presented here.

4. RESULTS

Stratigraphic profiles of measured $\delta^{44}Ca$, $\delta^{26}Mg$, $\delta^{13}C$, and $\delta^{18}O$ values, Sr/Ca, Mg/Ca ratios and mineralogy are shown in Figs. 2 and 5. Measured $\delta^{44}Ca$, $\delta^{26}Mg$, $\delta^{13}C$, and $\delta^{18}O$ values and Mg/Ca ratios for the subset of Clino samples that underwent gentle acid leaching to isolate dolomite are shown in Fig. 3. Measured $\delta^{44}Ca$ and $\delta^{26}Mg$ values for pore-fluids from Sites 1003 and 1007 (Ca only) are shown in Figs. 4 and 6.

4.1. Sediment Ca isotopes

At each studied site we observe stratigraphically coherent variability in bulk sediment $\delta^{44}Ca$ values, though the magnitude and structure of the variability varies significantly between sites (Fig. 2). For example, $\delta^{44}Ca$ values at Clino vary from −1‰ at 650–675 mbsf, to −0.6‰ at 540–550 mbsf, down to −1.4‰ between 290 and 320 mbsf then back up to −0.9‰ at 150 mbsf. In contrast, $\delta^{44}Ca$ values at Site 1131 sit at -1.10 ± 0.17‰ (2σ; $N = 44$) for the entire 550-m section. Measured $\delta^{44}Ca$ values from the LBB and Unda are also relatively uniform, though measured $\delta^{44}Ca$ values are on average ~0.6‰ higher (-0.53 ± 0.18‰, 2σ; $N = 27$) than the margin and slope sites (-1.13 ± 0.40‰, 2σ; $N = 253$). The total range in sediment $\delta^{44}Ca$ values from all studied sites is >1.2‰; the highest $\delta^{44}Ca$ values, up to −0.35‰, are found in dolomites from the LBB and Unda and lowest $\delta^{44}Ca$ values, ~−1.5‰, occur in near surface sediments from Sites 1003, 1007, and Clino. Minimum $\delta^{44}Ca$ values are similar to bank-top sediment from the GBB ($\delta^{44}Ca = -1.36 \pm 0.16$‰, 2σ; $N = 17$; Table S1) whereas maximum $\delta^{44}Ca$ values are ~0.8‰ higher than average pelagic carbonate sediments ($\delta^{44}Ca = -1.25 \pm 0.30$‰, 2σ; $N = 179$; (Fantle and Tipper, 2014; Gothmann et al., 2016)) and ~0.6‰ higher than bulk silicate Earth ($\delta^{44}Ca = -0.98$‰; (Fantle and Tipper, 2014)).

Sediment $\delta^{44}Ca$ values co-vary with the abundance of aragonite and Sr/Ca ratios in the sites from the Bahamas (Fig. 2). Sediments in the upper 100 m from Site 1007 and 1003 and between 280 and 320 mbsf at Clino contain up to 85 wt% aragonite and are characterized by Sr/Ca ratios >6 mmol/mol and $\delta^{44}Ca$ values between −1.22 and −1.56‰. The decline in aragonite abundance at Sites 1003, 1007 and Clino is associated with a decline in sediment Sr/Ca ratios and an increase in sediment $\delta^{44}Ca$ values peaking at ~200 and ~300 mbsf ($\delta^{44}Ca \sim -0.8$‰) at Sites 1003 and 1007, respectively, and 540–550 mbsf ($\delta^{44}Ca \sim -0.6$‰) at Clino. Bulk sediment $\delta^{44}Ca$ values at Sites 1003 and 1007 decline and Sr/Ca ratios increase below 200–250 mbsf, however, the shift is not accompanied by a significant increase in aragonite abundance. At all of the sites in the Bahamas, samples with the highest $\delta^{44}Ca$ values (up to −0.35‰) and lowest Sr/Ca ratios (down to ~0.16 mmol/mol) tend to be partly or fully dolomitized.

4.2. Pore-fluid Ca isotopes

Measured $\delta^{44}Ca$ values of sediment pore-fluids from Sites 1003 and 1007 are shown in Fig. 4. Both profiles are characterized by large declines in the pore-fluid $\delta^{44}Ca$ value within the upper 100 m, from the seawater value (0‰) to values characteristic of the bulk sediment (−1 to −1.2‰). Concentrations of Ca in the pore-fluid do not change appreciably in the upper ~100 mbsf of the sediment column at both sites, implying that the associated decline in pore-fluid $\delta^{44}Ca$ values is due to neomorphism and recrystallization of the carbonate sediments with little net dissolution or precipitation.

4.3. Sediment Mg isotopes

Measured $\delta^{26}Mg$ values of sediments from all studied sites occupy a fairly narrow range ($\delta^{26}Mg = -2.93 \pm 0.41$‰, 2σ; $N = 254$). The average $\delta^{26}Mg$ value for the shallow water sites (Clino, Unda, and LBB) is slightly higher ($\delta^{26}Mg = -2.83 \pm 0.29$‰, 2σ; $N = 103$) than the average $\delta^{26}Mg$ value ($\delta^{26}Mg = -3.01 \pm 0.42$‰, 2σ; $N = 146$) for slope sites (Sites 1003, 1007, and 1131) and bank-top sediment ($\delta^{26}Mg = -3.11 \pm 0.05$‰, 2σ; $N = 5$) but overall there is remarkably little variability considering the samples range from relatively unaltered mixtures of aragonite, high-Mg calcite, and low-Mg calcite to sediments that have undergone pervasive dolomitization. The lack of clear signals in bulk sediment $\delta^{26}Mg$ values related to changes in aragonite ($\delta^{26}Mg \sim -1.8$‰; (Wombacher et al., 2011; Wang et al., 2013)) abundance is conspicuous though it is likely due to the very low Mg content of aragonite (2–4 mmol Mg/mol Ca; (Morse and Mackenzie, 1990)) compared to all other carbonate phases (LMC, HMC and dolomite). The bulk sediment average Mg/Ca ratio (excluding dolomites from Clino, Unda, and LBB) is ~50 mmol/mol.

4.4. Pore-fluid Mg isotopes

The Mg isotopic composition of pore-fluids from Site 1003 (Fig. 6) is constant in the upper 62 m of the sediment column (avg. $= -0.78 \pm 0.07$‰, 2σ; $N = 10$) but increases abruptly thereafter, reaching a maximum value of +0.12‰ at 294 m. The increase in pore-fluid $\delta^{26}Mg$ values is accompanied by a decline in pore-fluid Mg

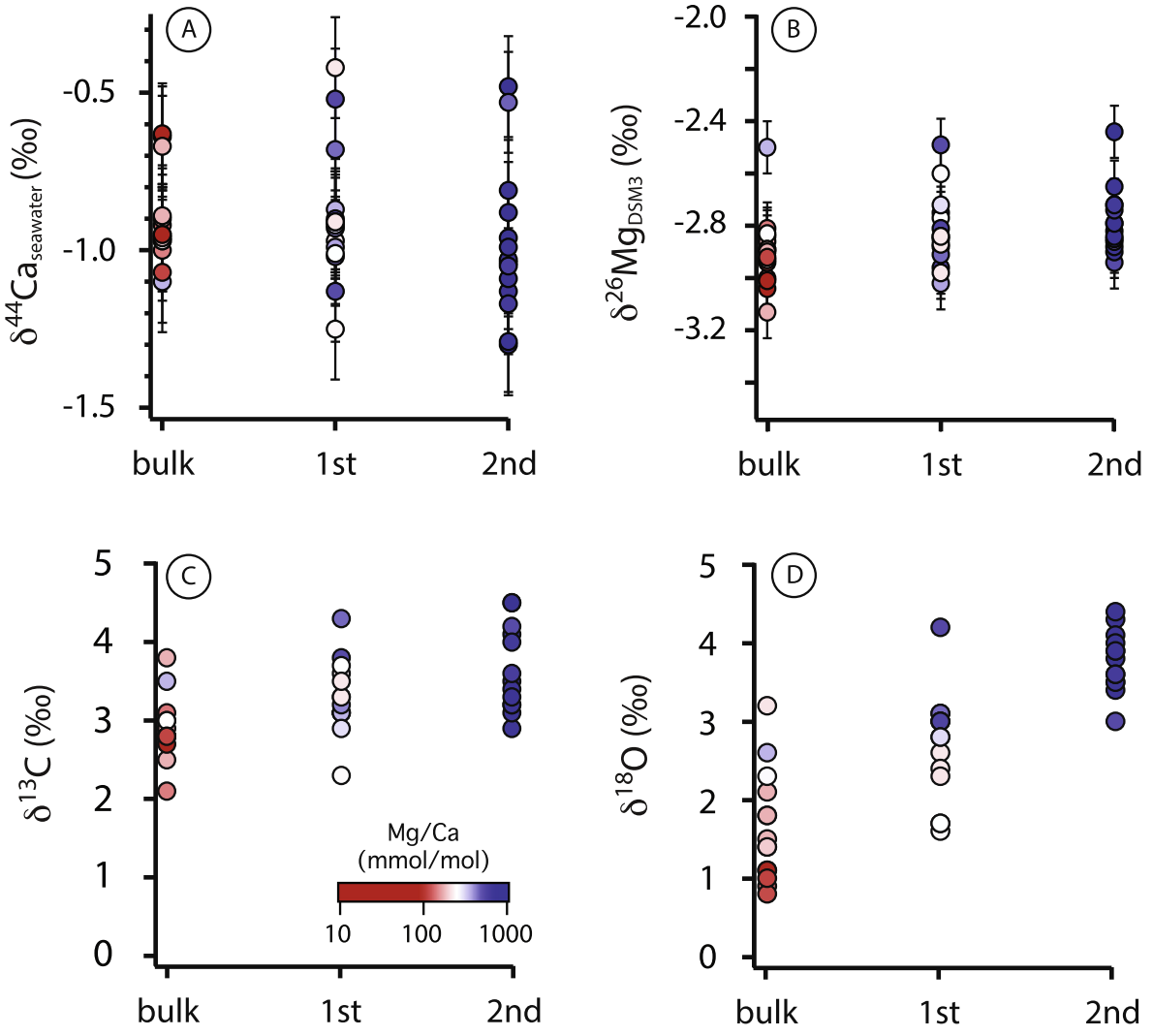

Fig. 3. Results from the dolomite leach experiments. (A) Measured $\delta^{44}Ca$ values for the leach experiments. Bulk, 1st, and 2nd denote bulk sample, 1st leach, and 2nd leach. Samples are colored based on sediment Mg/Ca ratio. Note that while the total range in sediment $\delta^{44}Ca$ values increases with sequential leaches, there is not a systematic shift in the measured $\delta^{44}Ca$ values; i.e. the diagenetic calcites and dolomites have similar $\delta^{44}Ca$ values. (B) Measured $\delta^{26}Mg$ values for the leach experiments. (C) Measured $\delta^{13}C$ values for the leach experiments. (D) Measured $\delta^{18}O$ values for the leach experiments. (For interpretation of the references to color in this figure legend, the reader is referred to the web version of this article.)

concentrations (Table S1) and an increase in the abundance of dolomite within the sediment column (though it remains a minor component; Fig. 2).

4.5. Dolomite leach experiments

Measured Mg/Ca ratios, $\delta^{18}O$, $\delta^{13}C$, $\delta^{44}Ca$, and $\delta^{26}Mg$ values for 15 leached samples from two depth intervals in Clino (367.10–379.06 mbsf and 495.90–648.66 mbsf) are shown in Fig. 3A-D. Sequential leaches produce samples with increasing dolomite content as shown by a systematic increase in sediment Mg/Ca ratios and $\delta^{18}O$ values ((Horita, 2014) Fig. 3C and D). In contrast, the average $\delta^{44}Ca$ value of the 15 samples is similar for all leach steps (−0.91‰, −0.89‰, and −0.98‰, respectively) indicating that sequential leaching and purification of the dolomite fraction is not associated with any systematic change in sediment $\delta^{44}Ca$ values (Fig. 3A). However, the total range in sediment $\delta^{44}Ca$ values does increase during sequential leaching from 0.5‰ in bulk sediments (−1.10‰ to −0.63‰) to 0.8‰ in leached sediments (−1.30‰ to −0.48‰). Average $\delta^{26}Mg$ values of the bulk and leached sediments (Fig. 3B) are indistinguishable from one another (−2.89‰, −2.82‰, and −2.78‰, respectively) and have a similar range of 0.6–0.7‰ (−2.4‰ to −3.1‰).

5. DISCUSSION

The process of transforming unlithified metastable carbonate minerals such as aragonite and high-Mg calcite into limestone and dolomite (diagenesis) involves chemical exchange between the solid and the local pore-fluid. The

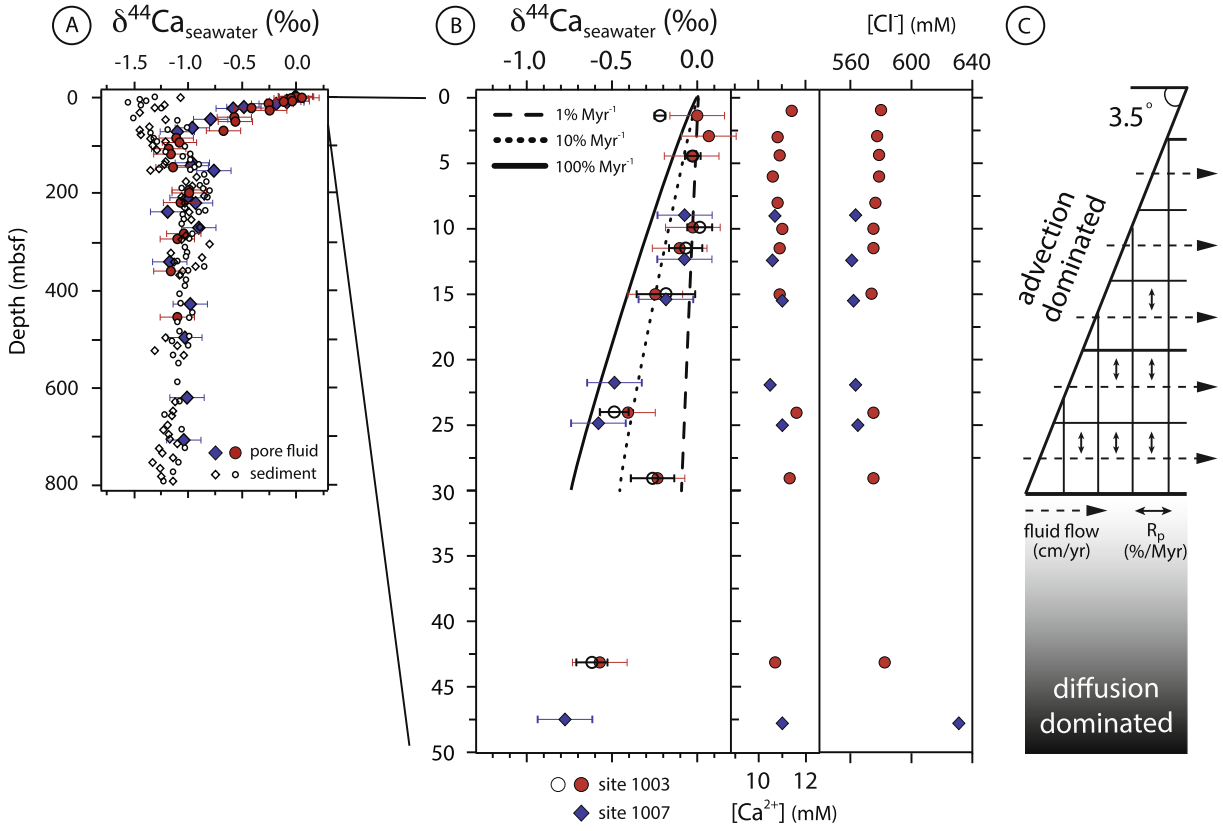

Fig. 4. Pore fluid and sediment $\delta^{44}Ca$ values, pore-fluid $[Cl^-]$ (in mM), and pore-fluid $[Ca^{2+}]$ from Sites 1003 and 1007. (A) Pore fluid (colored symbols) and bulk sediment (open symbols) $\delta^{44}Ca$ values for Sites 1003 and 1007. At both sites pore fluid $\delta^{44}Ca$ values decline from a seawater value (0‰) to $\delta^{44}Ca$ values indistinguishable from the host sediment over the upper ~100 m of the sediment column. Depth profiles of pore-fluid $\delta^{44}Ca$ values from slope Sites 1003 and 1007 (A and B) exhibit behavior that is similar to profiles from deep-sea sites (22, 55) in that pore-fluid $\delta^{44}Ca$ values decline over the first few tens of meters from a seawater value (0‰) to a $\delta^{44}Ca$ value indistinguishable from the carbonate sediment (−1 to −1.2‰) while concentrations of Ca in the pore-fluid remain relatively constant. These observations suggest, similar to studies in deep-sea sites (22, 55), that recrystallization and neomorphism in shallow-water carbonate sediments is associated with little Ca isotopic fractionation ($\alpha^{44/40}_{xtal-calcite/dolomite} \sim 0.9998$ to 1.0000) for the re-precipitated calcite or dolomite. (B) Pore-fluid $\delta^{44}Ca$ values, $[Ca^{2+}]$, and $[Cl^-]$ (in mM) in the upper 50 m at Sites 1003 and 1007. Open symbols are samples run at Cambridge University, all other samples were analyzed at Princeton. Depth-profiles of constant $[Cl^-]$ within this interval (not shown) are consistent with rapid (lateral) fluid flow. Declining pore-fluid $\delta^{44}Ca$ values and constant pore-fluid $[Ca^{2+}]$ indicates rapid recrystallization and/or neomorphism within this interval with little net precipitation or dissolution. We model this process using a 1D advection-reaction equation (see text for details). Model results for different recrystallization rates are shown as dashed, dotted, and solid lines. (C) Schematic of the 1D-advection reaction model of lateral fluid flow and recrystallization/neomorphism for the upper ~50 m at Sites 1003 and 1007. (For interpretation of the references to colour in this figure legend, the reader is referred to the web version of this article.)

extent to which the chemical composition of the initial sediment is preserved during these transformations depends on four factors: (1) the relative abundance of the element in the fluid and solid phases, (2) the partitioning of that elemental or isotopic system into the primary and diagenetic carbonate phases (i.e. aragonite vs. dolomite), (3) the amount or rate of diagenetic recrystallization or neomorphism and (4) the degree to which the diagenetic system was 'fluid-buffered' or 'sediment-buffered' for that particular elemental or isotopic system during recrystallization and/or neomorphism. Here a fluid-buffered (or open) diagenetic system refers to one where the chemical composition of the diagenetic phase largely reflects the chemical composition of the diagenetic fluid whereas in a sediment-buffered (or closed) diagenetic system the chemical composition of the diagenetic phase largely reflects the chemical composition of the primary sediment.

Differences in the relative abundance and partitioning of elements and isotopes between the fluid and the primary and diagenetic carbonate minerals mean that the conditions that lead to fluid-buffered and sediment-buffered recrystallization and/or neomorphsim are element specific. For example, recrystallization and/or neomorphism under one set of diagenetic conditions can be fluid-buffered for some elements (e.g. O isotopes) while at the same time being sediment-buffered for others (e.g. Ca and C isotopes). Under a different set of conditions diagenesis could be fluid-buffered for both Ca and O isotopes. For simplicity in this study we consider Ca in the bulk sediment as our element-of-reference for characterizing diagenetic conditions as being either fluid-buffered or sediment-buffered. Thus when we refer to diagenesis as having occurred under fluid-buffered or sediment-buffered conditions it should be

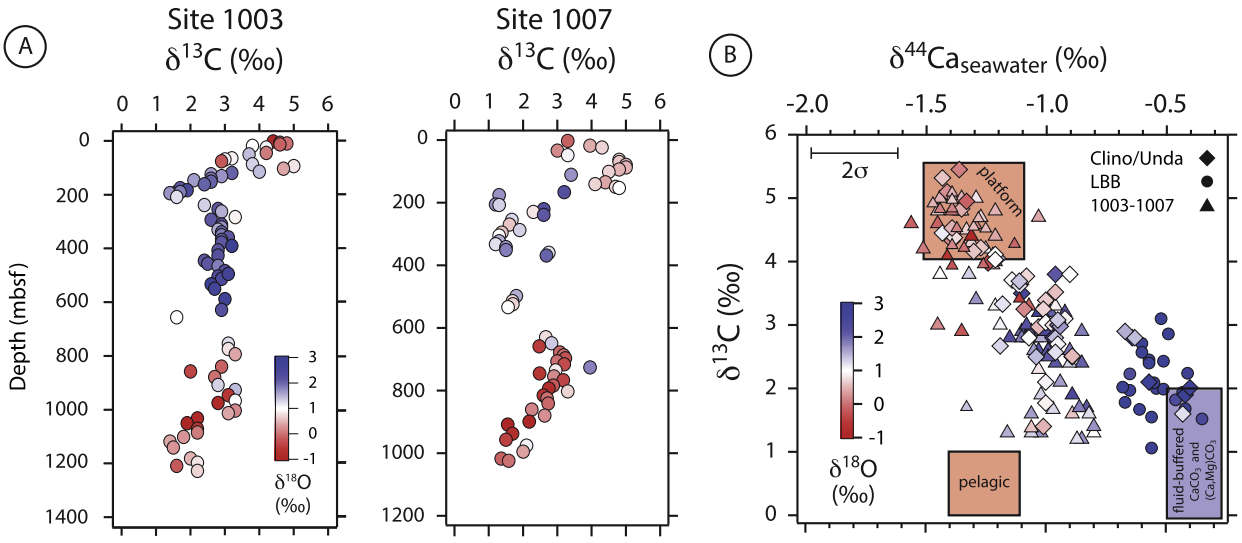

Fig. 5. Co-variation between bulk sediment $\delta^{13}C$ and $\delta^{44}Ca$ values at the Bahamas sites. (A) Depth profiles of $\delta^{13}C$ for Site 1003 (left) and 1007 (right). Samples are colored by measured $\delta^{18}O$ value. (B) Cross-plot of bulk sediment $\delta^{13}C$ and $\delta^{44}Ca$ values for Pliocene and Pleistocene-aged samples from the Bahamas. Samples are colored by measured $\delta^{18}O$ value. Approximately linear co-variation between sediment $\delta^{13}C$ and $\delta^{44}Ca$ values can be explained in large part by mixing high-$\delta^{13}C$ and low-$\delta^{44}Ca$ platform sources with low-$\delta^{13}C$ and high-$\delta^{44}Ca$ early diagenetic calcite and dolomite formed during recrystallization/neomorphism under fluid-buffered diagenetic conditions. Recrystallization/neomorphism under sediment-buffered conditions is not expected to change either bulk sediment $\delta^{13}C$ or $\delta^{44}Ca$ values. (For interpretation of the references to color in this figure legend, the reader is referred to the web version of this article.)

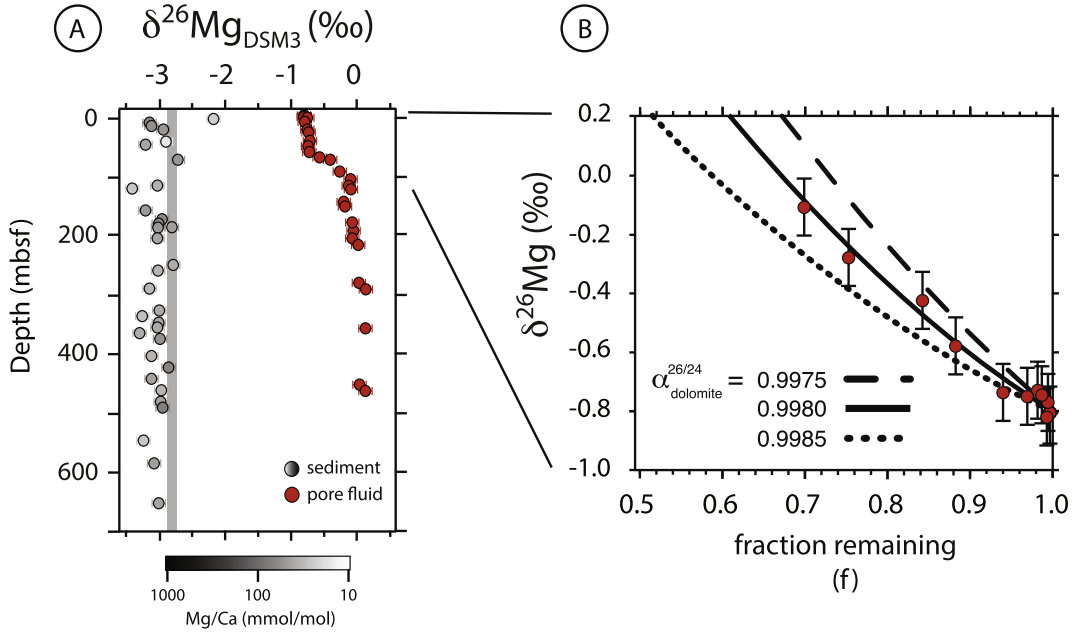

Fig. 6. (A) Pore-fluid and bulk sediment $\delta^{26}Mg$ values for Site 1003. The increase in pore-fluid $\delta^{26}Mg$ values at ~70 m depth is associated with a decline in pore-fluid $[Mg^{2+}]/[Cl^-]$ ratios (not shown; Table S1). The grey shaded line indicates the $\delta^{26}Mg$ value predicted for low-temperature dolomite under fluid-buffered conditions ($\alpha^{26/24}_{dolomite} \sim 0.9980$). (B) Model of pore-fluid Mg^{2+} and $\delta^{26}Mg$ values at Site 1003 assuming dolomite precipitation can be approximated by closed-system Rayleigh distillation and changes in pore-fluid $[Mg^{2+}]/[Cl^-]$ ratios. Dashed, dotted, and solid lines indicate different Mg isotope fractionation factors associated with dolomite precipitation.

interpreted as being with respect to Ca in the sediment unless otherwise specified.

With the notable exception of O, the isotopic composition of the major elements in carbonate minerals (Ca, C, and Mg in dolomite only) are thought to be relatively robust to alteration during diagenesis due to the high concentrations of these elements in the sediment compared to most diagenetic fluids. As a result, it is generally assumed

that diagenesis occurs under sediment-buffered conditions with respect to these elements. Although the assumption of sediment-buffered conditions appears to be generally valid for Ca in recrystallized carbonate-rich sediments in the deep-sea (Fantle and DePaolo, 2007), it has not been shown to be valid in shallow-water carbonate sediments.

5.1. An early diagenetic origin for stratigraphic variability in bulk sediment $\delta^{44}Ca$, $\delta^{26}Mg$ values and major/minor element chemistry

One of the most striking aspects of our data is that shallow water (<1000 mbsl) carbonate sediments from the toe-of-the-slope to the platform margin along the western flank of the Great Bahama Bank show coherent stratigraphic variability of up to 1‰ in bulk sediment $\delta^{44}Ca$ values, other major and minor element proxies (e.g. Sr/Ca ratios, $\delta^{13}C$, and $\delta^{18}O$ values) and mineralogy (Figs. 2, 4, and 5). Bulk sediments with low $\delta^{44}Ca$ values typically have high Sr/Ca ratios whereas sediments with high $\delta^{44}Ca$ values have low Sr/Ca ratios. Low bulk sediment $\delta^{44}Ca$ values also tend to be associated with high $\delta^{13}C$ values and low $\delta^{18}O$ values (Fig. 5). The relationship between bulk sediment $\delta^{44}Ca$ values and mineralogy is more complex – in the upper 200 m of Sites 1007, 1005, and 1003 the upper 400 m at Clino there is strong co-variation between bulk sediment mineralogy and $\delta^{44}Ca$ values with low $\delta^{44}Ca$ values associated with high wt% aragonite and with heavier $\delta^{44}Ca$ values associated with calcite and dolomite (Fig. 2). However, at both Sites 1003 and 1007, there is also a decline in $\delta^{44}Ca$ values below 200–400 m that is not accompanied by any change in bulk sediment mineralogy (i.e. the sediment is overwhelmingly calcite throughout) but is accompanied by an increase in sediment Sr/Ca ratios.

There are two processes capable of generating stratigraphic co-variation in bulk sediment geochemistry ($\delta^{44}Ca$, $\delta^{13}C$, $\delta^{18}O$, and Sr/Ca ratios) and mineralogy at the Bahamas sites. The first is mixing of sediment from different carbonate sources. One possibility is changes in production and/or transport of platform-top aragonite and high-Mg calcite. Measured $\delta^{44}Ca$ values for aragonite muds from NW Andros Island and ooids from Joulter Cays average −1.36‰ ($N = 14$; Table S1) whereas measured $\delta^{44}Ca$ values for high-Mg calcite are significantly higher (−0.8‰ to −0.9‰; Site 1131 and (Holmden et al., 2012)). However, mixing of these two end-members cannot explain the variability in bulk sediment $\delta^{44}Ca$ values as high-Mg calcite makes up only a small portion of the bulk sediment and there is no co-variation between sediment Mg/Ca and $\delta^{44}Ca$ values in the upper 200–300 m at Sites 1003 and 1007. In addition, mixing between aragonite and high-Mg calcite clearly cannot explain dolomite with $\delta^{44}Ca$ values >−0.5‰ at Clino, Unda, and the LBB.

Mixing of pelagic and platform sources of carbonate sediment is more likely to be an important source of stratigraphic variability in the geochemistry of bulk carbonate sediments for the more distal sites in this study (Sites 1003 and 1007). Previous work on stratigraphic variations in the $\delta^{13}C$ values and mineralogy of carbonate sediments on platform slopes in the Bahamas and other carbonate platforms by Swart (Swart and Eberli, 2005; Swart, 2008) argued that the ~4‰ decline in the $\delta^{13}C$ value of bulk carbonate sediments and loss of aragonite from the surface to ~200 mbsf (Fig. 5) could be explained largely by an increase in contributions from pelagic carbonate sources (with a $\delta^{13}C \sim 0$‰). Although we do not know the local $\delta^{44}Ca$ value of pelagic carbonate sources, the average $\delta^{44}Ca$ value of Cenozoic pelagic carbonates (foraminifera and nannofossils) is -1.25 ± 0.15‰ (1σ; $N = 179$; (Fantle and Tipper, 2014; Gothmann et al., 2016)), suggesting that mixing of carbonate sources (e.g. pelagic and platform) may explain some, but not all of the ~0.7‰ increase in bulk sediment $\delta^{44}Ca$ values between the sediment-water interface and 200–300 mbsf at Sites 1003 and 1007 (Fig. 5). This is supported by analyses of smear slides from the upper ~400 m at Site 1003 which indicate no systematic down-core changes in either relative grain size (sand/silt/clay) or composition (foraminifera/nannofossils/micrite) of the sediment (Eberli et al., 1997b). Increasing contributions from pelagic carbonate sources likely plays a more important role in explaining some of the shift to lower $\delta^{44}Ca$ values in Miocene-aged sediment below 200–400 mbsf at sites on the slope.

The second process capable of generating both stratigraphic variability and elevated bulk sediment $\delta^{44}Ca$ values is neomorphism and recrystallization of carbonate sediments that occurs under variable (fluid-buffered vs. sediment-buffered) diagenetic conditions. In particular, recrystallization and neomorphism under fluid-buffered conditions in marine sediments is expected to increase the $\delta^{44}Ca$ value of bulk carbonate sediments because (1) Ca isotope fractionation during calcite precipitation is rate-dependent (Fantle and DePaolo, 2007; Tang et al., 2008; DePaolo, 2011), approaching a value ($\alpha^{44/40}_{xtal\text{-}calcite}$) of ~0.9998 to 1.0000 at rates associated with early marine diagenesis in deep-sea sediments and (2) the diagenetic fluid is inferred to be relatively unaltered seawater with a $\delta^{44}Ca$ value of ~0‰. In contrast, recrystallization and neomorphism under sediment-buffered conditions is expected to result in little change in the bulk sediment $\delta^{44}Ca$ value as the majority of the Ca is inherited from the precursor sediment. As a result, temporal changes in sedimentary diagenetic conditions - for example a transient (geologically) increase in the extent of fluid-buffered diagenesis - should produce coherent stratigraphic variability in bulk sediment $\delta^{44}Ca$ values and other carbonate-bound geochemical proxies (i.e. $\delta^{13}C$, $\delta^{18}O$, and Sr/Ca ratios). In this case elevated $\delta^{44}Ca$ values should indicate sediments that have undergone more extensive recrystallization and/or neomorphism under fluid-buffered conditions. One of the advantages of invoking this process is that it neatly explains large enrichments in ^{44}Ca in carbonate sediments – i.e. $\delta^{44}Ca$ values as high as −0.3‰ – as the consequence of more extensive recrystallization and/or neomorphism under fluid-buffered conditions. In addition, because the chemical and isotopic composition of a fluid-buffered diagenetic carbonate is determined by the fluid and is independent of the precursor, it is effectively a second carbonate 'source' that will produce geochemical co-variation that is analogous to mixing of different carbonate sediments. Thus this process is also

capable of explaining observations of co-variation between bulk sediment $\delta^{44}Ca$ values, sediment mineralogy (aragonite abundance), and other geochemical proxies (e.g. $\delta^{13}C$, $\delta^{18}O$, and Sr/Ca ratios).

In contrast to the large stratigraphic variability observed in bulk sediment mineralogy and $\delta^{44}Ca$ values, measured $\delta^{26}Mg$ values at all sites show little coherent stratigraphic variability and, with few exceptions, fall within a relatively narrow range ($-2.8 \pm 0.5‰$; Fig. 2). Although the offset from seawater (~2‰) is similar to empirical estimates of fractionation factors for Mg-calcite from laboratory experiments at 20–30 °C (Li et al., 2012; Saulnier et al., 2012), the lack of variability in bulk sediment $\delta^{26}Mg$ values is surprising as $\delta^{26}Mg$ values in bulk carbonate sediments are relatively susceptible to diagenetic alteration – i.e. the low Mg content of the bulk sediment means that diagenesis almost always occurs under fluid-buffered conditions with respect sediment Mg (Higgins and Schrag, 2012). Previous studies have shown that recrystallization of low-Mg biogenic calcite in deep-sea sediments is associated with greater fractionation of Mg isotopes (i.e. $\alpha^{26/24}_{xtalcalcite} \sim 0.9950$; (Higgins and Schrag, 2012)) and carbonates with low $\delta^{26}Mg$ values (down to −3.91‰) have been measured in shallow water calcites from the Marion Plateau (Fantle and Higgins, 2014). Although we do not have a definitive explanation for the absence of samples with $\delta^{26}Mg$ values <−3.5‰ in the Bahamas or Site 1131 the most straightforward explanation is that this carbonate, if present, is swamped in bulk samples by the Mg in high-Mg calcite (in bank-top sediments; Table S1) or dolomite (in diagenetically stabilized carbonate sediments). Thus, the lack of stratigraphic variability in bulk sediment Mg isotopes can be attributed to very similar Mg isotope fractionation factors for both high-Mg calcite and dolomite (i.e. $\alpha^{26/24}_{Mgcalcite} \sim \alpha^{26/24}_{dolomite}$). This explains why neomorphism of mixtures of high-Mg calcite and aragonite to dolomite under fluid-buffered conditions leads to very little change in bulk sediment $\delta^{26}Mg$ values in spite of major changes in mineralogy and bulk sediment chemistry (i.e. $\delta^{44}Ca$, $\delta^{13}C$, and $\delta^{18}O$ values).

5.2. Fluid-buffered early marine diagenesis and bulk sediment $\delta^{44}Ca$ values

A surprising result of this study is the extent to which bulk sediment $\delta^{44}Ca$ values in shallow-water carbonate sediments appear to be affected by fluid-buffered early marine diagenesis. There are at least two processes likely to lead to early diagenetic recrystallization and neomorphism under fluid-buffered conditions for Ca; (1) a reduction in sedimentation rate or depositional hiatus that keeps shallow sediments at or near the seafloor for prolonged periods of time, and (2) fluid flow in shallow sediments driven by various external processes (differences in hydraulic head, compensation for freshwater flow, changes in eustatic sea-level, geothermal heating, density gradients due to evaporation, etc.). Both appear to play a role in creating fluid-buffered diagenetic conditions in the Bahamas. For example, the effects of reduced sedimentation rate can be seen in the elevated $\delta^{44}Ca$ values (up to −0.6‰) in partly dolomitized sediments in Clino below a prominent marine hardground at ~536 mbsf (Fig. 2). The hardground coincides with the late Miocene to early Pliocene and is interpreted to have developed from prolonged exposure in response to a decline in sediment supply from the platform (Kenter et al., 2001).

The role of fluid flow in maintaining fluid-buffered diagenetic conditions in shallow marine sediments is poorly quantified, though the role of fluid flow in the early marine diagenetic alteration of shallow water carbonate sediments is widely recognized. For example, almost all models (Hardie, 1987; Holland and Zimmerman, 2000) of early dolomitization include a source of fluid flow to supply the necessary Mg to turn calcium carbonate into dolomite (a *minimum* of 100 l of modern seawater is required to transform 1 kg of $CaCO_3$ into an equivalent number of moles of $Ca_{0.5}Mg_{0.5}CO_3$) but there are only a handful of observations of large-scale active fluid flow in modern shallow-water sedimentary systems. Fortunately, most of these observations come from studies of the Bahamas as part of ODP Leg 166 and the Bahamas Drilling Project (Eberli et al., 1997a; Henderson et al., 1999; Ginsburg, 2001). These studies indicate rates of lateral fluid flow ranging from 5 to 10 cm/yr for sediments on the Bahamas slope (ODP Site 1009) from depth profiles of pore-fluid chemistry ($^{234}U/^{238}U$ and $[Cl^-]$) and temperature. Depth profiles of pore-fluid $[Cl^-]$ at Sites 1003 and 1007 are similar to those studied by Henderson et al. (1999); constant seawater-like values in the upper 20–30 m followed by a linear increase down to 100 to 200 mbsf (Table S1). Temperature profiles at Sites 1007 and 1003 are also similar to those observed at other sites on Leg 166 (Eberli et al., 1997b) and consistent with significant fluid flow in the upper tens of meters of the sediment column; geotherms in the upper 30–80 m of the sediment are lower (Site 1007) or non-linear (Site 1003) when compared to geotherms deeper in the sediment column. As a result, though we do not have direct measurements of subsurface fluid flow at Sites 1003 and 1007, the pore-fluid chemistry and sediment temperature profiles are consistent with a zone of rapid fluid flow (5–10 cm/yr in the horizontal) in the upper ~25 m of the sediment column at both sites. Given the potential for additional sources or focusing of fluid flow on the platform top and margin (e.g. Clino, Unda, and LBB) these rates are likely minimum estimates for these sites. Although the exact mechanism behind the fluid flow observed in shallow sediments from sites on the continental slope in the Bahamas remains uncertain, numerical models indicate that the rates of fluid flow within a carbonate platform on the order of cm/yr can be achieved through multiple means. Examples include geothermal convection, glacial-eustatic variations in sea-level, interactions between seawater and meteoric groundwater, and brine reflux (Kaufman, 1994; Caspard et al., 2004; Jones et al., 2004; Garcia-Fresca et al., 2012).

Given the high rates of lateral fluid flow in the upper tens of meters of the sediment column at Sites 1003 and 1007 it is surprising that at both sites the $\delta^{44}Ca$ value of the pore-fluid declines with depth in this interval (Fig. 4B). We attribute this decline to a longer path-length (and hence longer residence time) for fluids flowing laterally at greater depths in the sediment column leading

to more Ca isotopic exchange between the pore-fluid and sediment due to recrystallization and neomorphism. To explore this hypothesis we constructed a simple model for this process which assumes that the observed δ^{44}Ca profiles of the pore-fluid reflects the local balance between lateral fluid flow (U in cm/yr) and recrystallization and/or neomorphism:

$$\frac{d(\delta^{44}Ca_{f-out}\cdot M^{Ca}_{f-out})}{dt} = U\cdot(\delta^{44}Ca_{f-in}\cdot M^{Ca}_{f-in} - \delta^{44}Ca_{f-out}\cdot M^{Ca}_{f-out}) - R_p \cdot M^{Ca}_{sed}\cdot(\delta^{44}Ca_{f-out}+\varepsilon^{44}_{xtal}) + R_d\cdot M^{Ca}_{sed}\cdot\delta^{44}Ca_{sed} \quad (1)$$

where $\delta^{44}Ca_{f-in/out}$ is the Ca isotopic composition of the incoming/outgoing fluid, $M^{Ca}_{f-in/out}$ is the mass of Ca in the incoming/outgoing fluid (in mol), M^{Ca}_{sed} is the mass of Ca in the carbonate sediment, $\varepsilon^{44}_{xtal} = (\alpha^{44/40}_{xtal-calcite}-1)\cdot 10^3$ is the Ca isotopic fractionation factor associated with recrystallization and neomorphism, $R_{p,d}$ is the rate of mineral precipitation and dissolution associated with recrystallization and neomorphism (in %/Myr), and $\delta^{44}Ca_{sed}$ is the Ca isotopic composition of the bulk sediment. To simplify this equation further we make two additional assumptions: (1) local isotopic steady-state (i.e. $\frac{d(\delta^{44}Ca_{fluid}\times M^{Ca}_{fluid})}{dt}=0$) and (2) the concentration of Ca is equal to that of seawater and does not change along the path of fluid flow ($M^{Ca}_{f-in}=M^{Ca}_{f-out}=M^{Ca}_{seawater}$ and $R_p=R_d$). The first assumption is reasonable given the relatively short residence times of fluids in the upper 25 m (at most 4–8 kyr for a flow rate of 5–10 cm/yr and a continental slope dip of 3.5°) and the proposed timing of the current fluid flow regime (Holocene flooding of the platform top at ~6 kyr; (Droxler et al., 1983)). The second assumption is based on observations that the concentration of Ca in the pore-fluid at both sites 1003 and 1007 remains at the seawater value throughout the interval from 0 to >25 mbsf. This reduces Eq. (1) to:

$$\delta^{44}Ca_{f-out} = \frac{U\cdot\delta^{44}Ca_{f-in}\cdot M^{Ca}_{seawater} + R_p\cdot M^{Ca}_{sed}\cdot(\delta^{44}Ca_{sed}-\varepsilon^{44}_{xtal})}{U\cdot M^{Ca}_{seawater}+R_p\cdot M^{Ca}_{sed}} \quad (2)$$

Eq. (2) can then be solved iteratively for each box along the path length given rates of fluid flow (U) and recrystallization/neomorphsim (R_p) and given the boundary condition $\delta^{44}Ca_{f-in}=\delta^{44}Ca_{seawater}$ at the sediment-water interface. The path length (i.e. number of boxes) for each depth in the sediment column is calculated assuming a 3.5° dip of the continental slope (Fig. 4C). For rates of lateral fluid flow of 10 cm/yr, fitting the pore-fluid profiles of δ^{44}Ca values at both Sites 1003 and 1007 (Fig. 4B) requires rates of recrystallization and/or neomorphism on the order of 10%/Myr. These rates are on the high end of estimates based on recrystallization in deep-sea carbonate sediments (~1%/Myr; (Richter and DePaolo, 1987; Fantle and DePaolo, 2007)) but are consistent with the million-year timescales estimated for diagenetic alteration and dolomitization of platform carbonates in the Bahamas using ^{87}Sr/^{86}Sr isotopes (Vahrenkamp et al., 1988, 1991a).

5.3. Sediment-buffered early marine diagenesis and bulk sediment δ^{44}Ca values

Perhaps less surprising is the Ca isotope evidence for sediment-buffered recrystallization and neomorphism from sites on the slope in the Bahamas (Sites 1003 and 1007) and Site 1131 (Australia). We identify bulk carbonate sediments as having undergone sediment-buffered diagenesis with respect to Ca when they are composed predominately of low-Mg calcite and dolomite and yet are characterized by δ^{44}Ca values that approach or equal surface-sediment δ^{44}Ca values and have high Sr/Ca ratios (i.e. 3–7 mmol/mol). Note that in the Bahamas this implies sediment δ^{44}Ca values of −1.2 to −1.5‰ for sediment-buffered diagenesis of aragonite, whereas at Site 1131 sediment-buffered diagenesis of high-Mg calcite predicts a δ^{44}Ca value closer to −1‰ (Fig. 2). At Sites 1003 and 1007, sediment-buffered diagenesis is one potential explanation for the return to lower δ^{44}Ca values (and higher Sr/Ca ratios) below 200–300 m, though increasing contributions from pelagic sources with low δ^{44}Ca values also likely plays a role. At Site 1131 sediment-buffered diagenesis appears to dominate the entire sediment column. In contrast to sites in the Bahamas, pore-fluid Cl^- profiles at Site 1131 increase linearly with depth from the sediment-water interface, consistent with (present-day) diffusion-limited transport and persistent sediment-buffered diagenetic conditions at this site.

5.4. Using paired Mg and Ca isotopes to fingerprint dolomitization

The presence of large volumes of dolomitized carbonate sediments in the geologic record has long vexed geologists and geochemists as it is a rare mineral in modern and recent shallow-water environments and difficult to precipitate in the laboratory at low temperatures (Hardie, 1987; Land, 1998; Holland and Zimmerman, 2000). One of the few things that is agreed upon with regard to massive sedimentary dolomites is that they require a large source of Mg that can be supplied rapidly on million-year timescales. One possibility is diffusion from seawater (Compton and Siever, 1986; Blättler et al., 2015). Another is Mg supplied by fluid flow in sedimentary pore-fluids (Kaufman, 1994; Jones et al., 2004). Although not mutually exclusive, these two modes of Mg supply predict distinct signatures for the δ^{26}Mg and δ^{44}Ca value of the precipitated dolomite. For example, dolomitizing systems where the supply of Mg occurs exclusively by diffusion will tend to result in Rayleigh-type distillation of Mg in the pore-fluid and dolomites with more positive and variable δ^{26}Mg values (Blättler et al., 2015). Under these conditions the Ca that ends up in the dolomite will largely consist of Ca from any precursor carbonate sediment plus a smaller amount from the dolomitizing fluid. We regard this type of dolomite as having formed under sediment-buffered conditions as it preserves the δ^{44}Ca and δ^{13}C values of the primary sediment.

Alternatively, in systems where Mg supply is rapid relative to rates of consumption by dolomitization the

geochemical signature of the dolomite will reflect fluid-buffered conditions for all elemental and isotopic systems. In this case dolomite δ^{26}Mg values will be low and homogeneous, reflecting precipitation from an unaltered dolomitizing fluid with a fractionation factor ($\alpha^{26/24}_{dolomite}$) of ~0.9980 (Higgins and Schrag, 2010; Fantle and Higgins, 2014). Sediment δ^{44}Ca values should similarly reflect fluid-buffered diagenesis and will approach the value predicted for calcite precipitation at these slow rates (i.e. $\alpha^{44/40}_{dolomite} \sim 0.9998–1.0000$; (Fantle and DePaolo, 2007; Jacobson and Holmden, 2008; Turchyn and DePaolo, 2011)). Assuming the fluid is relatively unaltered seawater ($\delta^{44}Ca = 0‰$), this would result in dolomites that are enriched in ^{44}Ca compared to the primary carbonate sediment.

The magnitude of Mg and Ca isotope fractionation ($\alpha^{26/24}_{dolomite}$ and $\alpha^{44/40}_{dolomite}$) associated with dolomite precipitation at low temperatures (5–35 °C) is one of the main sources of uncertainty in using paired measurements of Mg and Ca isotopes to fingerprint the style of dolomitization (sediment-buffered vs. fluid-buffered). For Mg isotopes, previous studies on deep-sea sediment pore-fluid systems actively precipitating authigenic dolomite indicate $\alpha^{26/24}_{dolomite} \sim 0.9973–0.9980$ (Higgins and Schrag, 2010; Fantle and Higgins, 2014). Significantly smaller Mg isotope fractionation factors ($\alpha^{26/24}_{dolomite} > 0.9999$) have been inferred from studies of modern sabka dolomites (Geske et al., 2015a., 2015b), though sabhka dolomites slightly older in age (Pleistocene) suggest $\alpha^{26/24}_{dolomite} \sim 0.9987–0.9984$. We suspect that much of this variability is due to later re-setting under fluid-buffered vs. sediment-buffered conditions, though we note that characterizing Mg isotope fractionation in sabka-like dolomitizing systems is significantly more complicated due the presence of multiple Mg-bearing minerals (carbonates, evaporites and clay minerals). Consideration of the pore-fluid δ^{26}Mg and Mg/Cl profiles from Site 1003 results in an estimate for $\alpha^{26/24}_{dolomite}$ of 0.9980 assuming the changes can be modeled as Rayleigh fractionation (Fig. 6). Given the greater complexity associated with reconstructing Mg isotope fractionation in heterogeneous deep-sea sediments (Higgins and Schrag, 2010) and a weak temperature dependence (~1‰ decline in $\alpha^{26/24}_{dolomite}$ between 0 and 250 °C (Li et al., 2015)), the estimate from Site 1003 of $\alpha^{26/24}_{dolomite} \sim 0.9980$ is preferred for dolomitization of shallow-water carbonate sediments. For Ca isotopes the determination of $\alpha^{44/40}$ for dolomite precipitation is more difficult to discern from sediment pore-fluid systems because it occurs in conjunction with the precipitation of diagenetic calcite. Pore-fluid δ^{44}Ca profiles from Sites 1003 and 1007 both indicate $\alpha^{44/40}_{dolomite} \sim 0.9998–1.0000$ for all forms of carbonate diagenesis (recrystallization, neomorphism, and dolomitization; Fig. 4). In addition, the dolomite leach experiments showed no resolvable difference in bulk sediment δ^{44}Ca values as a function of dolomite content (in spite of an overall range in δ^{44}Ca values between samples of ~0.7‰; Fig. 3), suggesting that both the calcite and dolomite endmembers have similar δ^{44}Ca values (i.e. $\alpha^{44/40}_{dolomite} \sim \alpha^{44/40}_{xtalcalcite}$). Consequently, we tentatively assume that $\alpha^{44/40}_{dolomite} \sim 0.9998–1.0000$ for the formation of low-temperature dolomite, in agreement with (Holmden, 2009).

Both the dolomite leach experiments and bulk samples from Clino, Unda, and the LBB show some co-variation between δ^{26}Mg and δ^{44}Ca values with higher δ^{26}Mg values generally associated with lower δ^{44}Ca values (Fig. 7 – inset; Fig. 8). Overall, however, the measured δ^{26}Mg values of the Bahamas dolomites are low (−2.5‰ to −3‰) and have a relatively narrow distribution when compared to the range in δ^{26}Mg values observed in authigenic dolomites from the Miocene Monterey Fm. (Fig. 7; (Blättler et al., 2015)). Sediment δ^{44}Ca values span a range of almost 1‰, from −1.3 to −0.35‰, a range that is similar to that observed in the dolomites from the Monterey Fm. However, the majority of the dolomite samples from the Bahamas have δ^{44}Ca values higher than −0.7‰, whereas in the Monterey Fm most samples have δ^{44}Ca values lower than −0.7‰. Given these observations - low and homogeneous δ^{26}Mg value and high δ^{44}Ca values - the paired Mg and Ca isotope measurements indicate that dolomitization in the Bahamas was largely fluid-buffered. This conclusion agrees with previous studies that have argued based on sediment δ^{18}O values and petrography that the fluid responsible for dolomitization at Clino/Unda and the LBB was relatively unaltered seawater (Vahrenkamp et al., 1991b; Swart and Melim, 2000).

But do the dolomites from Clino, Unda, and the LBB represent a fully fluid-buffered endmember? For Mg isotopes, the average value of the Bahamas dolomites is $-2.84 \pm 0.26‰$ (2σ; $N = 41$), similar to platform dolomites measured in a previous study ($\delta^{26}Mg = -2.68 \pm 0.13‰$ 2σ; $N = 7$, (Fantle and Higgins, 2014)) and minimum δ^{26}Mg values measured in the authigenic dolomites of the Monterey Fm. (Fig. 7). This is almost exactly the expected offset given seawater as the dolomitizing fluid with δ^{26}Mg value of −0.82‰ ($\delta^{26}Mg_{fluid} = \delta^{26}Mg_{seawater}$) and $\alpha^{26/24}_{dolomite} = 0.9980$. For Ca isotopes the situation is less clear as the dolomite δ^{44}Ca values span a ~1‰ range. However, even the most ^{44}Ca-enriched dolomites are ~0.2‰ lower than the δ^{44}Ca value expected for $\alpha^{44/40}_{dolomite} = 0.9998$ to 1.000 and seawater as the dolomitizing fluid ($\delta^{44}Ca = 0‰$). This result suggests that either $\alpha^{44/40}_{dolomite} < 0.9998$ for low-temperature dolomite or that dolomitization occurred in conditions that were not fully fluid-buffered for sediment Ca (i.e. $\delta^{44}Ca_{fluid} < \delta^{44}Ca_{seawater}$). Observations of δ^{44}Ca values lower than seawater (0‰) in sedimentary pore-fluids within the zone of active fluid flow at Sites 1003 and 1007 (Fig. 4) is consistent with the latter hypothesis.

The presence of dolomite leachates from Clino with δ^{44}Ca values as low as −1.3‰ and the mild co-variation between sediment δ^{44}Ca and δ^{26}Mg values (Fig. 7 – inset; Fig. 8) suggest that dolomitization in the Bahamas can also be sediment-buffered. Mixing of fluid-buffered and sediment-buffered dolomites has been proposed as an explanation for the co-variation in δ^{44}Ca and δ^{26}Mg values in the Monterey Fm. (Fig. 7). In that case the difference between fluid-buffered and sediment-buffered conditions is related to the depth of dolomite precipitation within the shallow sediment column; dolomite precipitated near the sediment-water interface has a fluid-buffered composition whereas

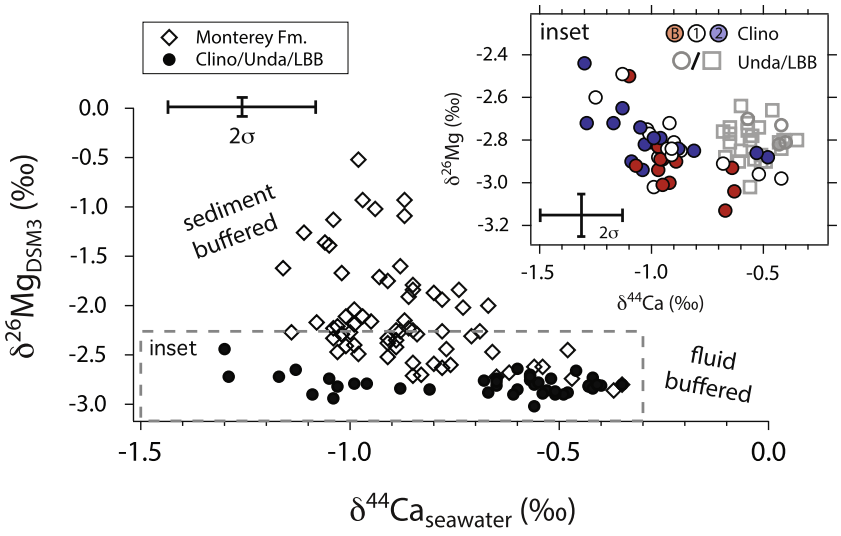

Fig. 7. Plot of paired $\delta^{26}Mg$ and $\delta^{44}Ca$ values of bulk sediment and leached samples from Clino, Unda, and the LBB. Also shown are samples from the Monterey Fm from Blättler et al. (2015). Dolomites precipitated under sediment-buffered conditions are associated with low $\delta^{44}Ca$ values (inherited from the precursor carbonate) and high (and variable) $\delta^{26}Mg$ values due to distillation of pore-fluid Mg^{2+}. Dolomites precipitated under fluid-buffered conditions will have relatively low and homogeneous $\delta^{26}Mg$ values and $\delta^{44}Ca$ values that are high (and variable). **INSET:** Measured $\delta^{26}Mg$ and $\delta^{44}Ca$ values for Bahamas dolomites. Dolomite leachates are labeled B (bulk), 1, and 2. Modest co-variation between $\delta^{26}Mg$ and $\delta^{44}Ca$ values from Clino indicate dolomitization under both fluid-buffered and sediment-buffered conditions at this site. Dolomites from Unda and the LBB appear to have formed under predominantly fluid-buffered conditions.

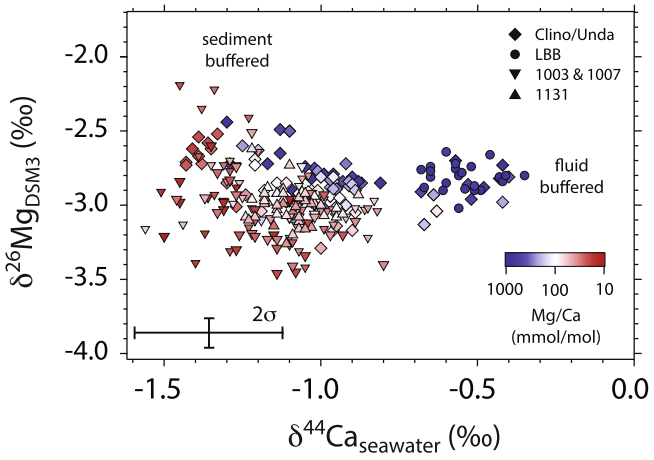

Fig. 8. Paired measurements of $\delta^{26}Mg$ and $\delta^{44}Ca$ values for carbonate sediments from all sites. Samples are colored based on Mg/Ca ratio. Note the range of $\delta^{26}Mg$ and $\delta^{44}Ca$ values associated with dolomites (Mg/Ca ~ 1000) reflecting dolomitization under both fluid-buffered and sediment-buffered conditions. (For interpretation of the references to colour in this figure legend, the reader is referred to the web version of this article.)

dolomite precipitated deeper in the sediment column is sediment-buffered with respect to Ca (Blättler et al., 2015). In contrast to the Bahamas, sediment-buffered conditions appear to dominate in the Monterey Fm. as only a handful of the samples have $\delta^{44}Ca$ values $>-0.7‰$ and $\delta^{26}Mg$ values $<-2.6‰$. This result is perhaps not surprising given the importance of fluid flow in shallow-water carbonate sediments but emphasizes the fundamental role it plays in determining fluid-buffered vs. sediment-buffered conditions during carbonate diagenesis.

In summary, paired measurements of Mg and Ca isotopes in marine dolomites can be used to fingerprint whether dolomitization occurred in a diagenetic environment that was fluid-buffered or sediment-buffered with respect Ca. Dolomites that are fluid-buffered are predicted to have relatively uniform $\delta^{26}Mg$ values that are ~2‰ lower than seawater and $\delta^{44}Ca$ values that approach the $\delta^{44}Ca$ value of seawater (0‰). In contrast dolomites that precipitate under sediment-buffered conditions are predicted to have variable and high $\delta^{26}Mg$ values due to distil-

lation of Mg in the dolomitizing fluid and $\delta^{44}Ca$ values that are inherited from the precursor carbonate sediment (−1 to −1.5‰). Using this fingerprint, we identify the massive shallow burial dolomites observed in the Bahamas at Clino, Unda, and the LBB as originating in a diagenetic environment that was predominantly (but not exclusively) fluid-buffered with respect to sediment Ca. This result complements observations of Mg and Ca isotopes in authigenic dolomites of the Monterey Fm. a very different dolomite-forming environment that nevertheless has a Mg and Ca isotope fingerprint that can be interpreted using the same diagenetic (fluid-buffered vs. sediment-buffered) framework and isotopic fractionation factors ($\alpha^{26/24}_{dolomite}$ and $\alpha^{44/40}_{dolomite}$). Applied to ancient dolomites this approach could yield estimates of paleo-seawater $\delta^{26}Mg$ and $\delta^{44}Ca$ values (most easily through the identification of the fluid-buffered end-members) and will aid in the more general characterization of the environmental information stored in the geochemistry of dolomitized carbonate sediments.

5.5. Mineralogy, early marine diagenesis, and the geochemistry of shallow-water sedimentary carbonates

Marine carbonate sediments serve as both direct (through the burial of the major elements Ca, Mg, and C), and indirect (as archives of information on temperature and seawater chemistry) records of the global carbon cycle over Earth history. Prior to the Mesozoic, it is thought that most carbonate sediments were deposited in shallow-water platform, shelf, and slope environments (Opdyke and Wilkinson, 1988; Boss and Wilkinson, 1991; Holmden et al., 1998; Ridgwell, 2005). Although these sediments are now mostly composed of calcite and dolomite there is substantial geochemical and petrographic (Sandberg, 1983) evidence that the primary carbonate minerals deposited included metastable forms such as aragonite and high-Mg calcite. While it is widely recognized that all carbonate sediments undergo diagenesis (Ginsburg, 1957; Berner, 1966; Walter et al., 1993; Patterson and Walter, 1994; Schrag et al., 1995; Melim et al., 2001), the extent to which the bulk and trace element geochemistry of the primary sediment is preserved during the transformation from unlithified sediment into rock is poorly known and widely debated (Swart, 2008; Knauth and Kennedy, 2009; Derry, 2010; Schrag et al., 2013; Husson et al., 2015). The data presented here indicate that paired measurements of Mg and Ca isotopes can be used to identify mineralogical changes (aragonite to calcite/dolomite) and characterize diagenetic environments (fluid-buffered vs. sediment-buffered) in ancient carbonate sediments. When applied to Neogene carbonate sediments from the platform, margin, and slope of the Great and Little Bahama Banks, paired measurements of Mg and Ca isotopes provide clear evidence of the role of both mineralogy and early marine diagenesis in determining the chemical composition and its stratigraphic expression in shallow-water carbonate sediments preserved in the rock record.

First, bulk sediment and pore-fluid chemistry from sites throughout the Bahamas indicate that active fluid-buffered carbonate diagenesis occurs in shallow sediments from the platform-top down the slope to at least ~650 m water depth. This fluid-buffered early marine diagenesis appears to be associated with the conversion of aragonite and high-Mg calcite to low-Mg calcite and dolomite and results in extensive chemical exchange between sediment and the diagenetic fluid. In particular, the large increases in bulk sediment $\delta^{44}Ca$ values we observe (up to 1‰ within Clino) require almost full recrystallization or neomorphism of the carbonate sediment under diagenetic conditions that would lead to the wholesale resetting of bulk sediment chemistry ($\delta^{44}Ca$, $\delta^{13}C$, $\delta^{26}Mg$, $\delta^{18}O$, Mg/Ca, Sr/Ca, $\delta^{238/235}U$, $\delta^{7}Li$, $\delta^{11}B$, etc.). Although fluid-buffered carbonate diagenesis is often associated with dolomitization, it can also occur as neomorphism of aragonite to calcite or simply calcite recrystallization.

Second, given that early marine diagenesis can occur under either fluid-buffered or sediment-buffered conditions, temporal changes in the style of diagenesis can produce stratigraphically coherent variability in major and minor element chemistry that can be reproduced regionally and perhaps globally. For example, at Sites 1003 and 1007, the depth profile in bulk sediment $\delta^{44}Ca$ values indicates a maximum near 200 mbsf or >100 m below the zone of present-day active fluid flow and fluid-buffered diagenesis. One explanation for this offset is that rates of fluid flow and the extent of fluid-buffered diagenetic alteration have changed systematically with time such that when the sediments near 200 m were initially deposited, fluid flow and the extent of fluid-buffered diagenetic alteration in the upper meters to 10's of meters of the sediment column were at a maximum (and much higher than today). Lower rates of fluid flow both before and after would be associated with increasingly sediment-buffered diagenetic conditions, the net result being a pronounced positive excursion in bulk sediment $\delta^{44}Ca$ values centered around the time of maximum fluid flow (and fluid-buffered diagenesis). Although the drivers of sedimentary fluid flow in the Bahamas remain unknown, glacial-eustatic sea-level changes are often cited as a likely source of sedimentary fluid flow in carbonate platforms (Kaufman, 1994; Swart and Melim, 2000) and offer a tantalizing link between global processes (changes in Earth's ice volume) and variations in the local early marine diagenesis of carbonate platforms.

5.5.1. Implications for stratigraphic variations in shallow-water $\delta^{13}C$ and $\delta^{18}O$ values over the Neogene

The conclusion that the stratigraphic variability in bulk sediment $\delta^{44}Ca$ values in the Bahamas is related in large part to the extent of fluid-buffered vs. sediment-buffered diagenetic alteration of platform aragonite has direct implications for the interpretation of the observed stratigraphic variability in bulk sediment $\delta^{13}C$ and $\delta^{18}O$ values and other geochemical proxies (e.g. Sr/Ca, Fig. 2) in both modern and ancient shallow-water carbonate sediments. In a previous study, Swart (2008) pointed out that carbonate sediments from platform margins around the world (Bahamas, Australia, and Maldives) all show a similar increase in bulk sediment $\delta^{13}C$ values over the Neogene that are de-coupled from changes in the global carbon cycle. Swart (2008) argued that the increases in shallow water carbonate $\delta^{13}C$

values could be explained as a mixture of a pelagic source with a $\delta^{13}C$ value of ~0‰ and a platform (aragonite) source with a $\delta^{13}C$ value of +4–5‰ with increasing contributions from the platform source over the Neogene. Our results do not contradict this hypothesis, but suggest that a significant fraction of stratigraphic increase in bulk sediment $\delta^{13}C$ values could also be explained by changes in the extent of diagenetic alteration of aragonite to calcite under fluid-buffered conditions with relatively unmodified seawater ($\delta^{13}C \sim 0‰$, $\delta^{18}O \sim 0‰$, temperature = 12–16 °C) in the uppermost 10's of meters of the sediment column (e.g. Fig. 5). The identification of fluid-buffered diagenesis, in particular spatial and temporal variations in the extent of fluid-buffered vs. sediment-buffered diagenesis, as an alternative mechanism for generating stratigraphic variability in the geochemistry of bulk carbonate sediments is significant because this phenomenon is likely to have been common in the shallow-water carbonate sediments that constitute the bulk of the pre-Mesozoic carbonate rock record.

Our interpretation that sediment-buffered diagenesis dominates below 500–800 m at Sites 1003 and 1007 and over the entirety of Site 1131 predicts that the $\delta^{13}C$ values of these sediments should reflect the primary precipitates (aragonite and high-Mg calcite for 1003/1007 and 1131, respectively). At Sites 1003 and 1007, the $\delta^{13}C$ values of these sediment-buffered neomorphosed aragonites are only between +2 to +3‰, or ~1–2‰ more negative than the $\delta^{13}C$ of modern bank-top sediment (+4 to +5‰ (Swart et al., 2009); Table S1). This could be due in part to greater contributions of pelagic sources to Miocene sedimentation at these sites, but it may also be due to an increase in the $\delta^{13}C$ value of platform aragonite between the Miocene and the Pliocene. Bulk sediment $\delta^{13}C$ values at Site 1131 occupy a narrow range from +1 to +2‰ but span only the Pliocene and Pleistocene.

5.5.2. Implications for the preservation of minor and trace elements proxies in ancient shallow-water carbonate sediments

Early marine diagenesis that is capable of both resetting the chemical and isotopic composition of bulk carbonate sediments on million-year timescales and changing from fluid-buffered to sediment-buffered within a stratigraphic column poses a significant challenge for the application of many minor and trace element proxies to ancient carbonate sediments. Given the relative diagenetic stability of bulk sediment $\delta^{44}Ca$ and $\delta^{13}C$ values, the observation that variations in fluid-buffered early marine diagenesis can produce large (~1‰ and 4‰, respectively) changes in bulk sediment $\delta^{44}Ca$ and $\delta^{13}C$ values suggests that all minor and trace element proxies in fluid-buffered carbonate sediments will reflect the chemistry of the early diagenetic fluid. However, our results also provide a tool for identifying carbonate sediments lithified under largely sediment-buffered diagenetic conditions where minor and trace elements in the primary carbonate sediment are more likely to be preserved. Although an exhaustive review of carbonate-bound geochemical proxies is also beyond the scope of this study, there are at least three factors that will determine the extent to which these proxies are complicated and/or compromised by variations in mineralogy and fluid-buffered vs. sediment-buffered diagenesis.

First, as these proxies are by their nature based on minor and trace constituents of sedimentary carbonate minerals, they tend to be regarded as susceptible to diagenesis in particular if the abundance of the minor or trace element is high in early diagenetic fluids compared to the bulk sediment. Although this does not guarantee that a proxy will be sensitive to diagenesis due to the potential for offsetting effects associated with partition coefficients and isotopic fractionation factors, it is a key boundary condition in determining proxy behavior during carbonate diagenesis (Banner and Hanson, 1990; Marshall, 1992). Most trace element proxies should be more sensitive to fluid-buffered diagenetic alteration than major elements like C and Ca. This can be shown for Sr/Ca for depths below 500–800 m at Sites 1003 and 1007; despite bulk sediment $\delta^{44}Ca$ values that are indistinguishable from surface sediments, Sr/Ca ratios never recover to surface sediment values of ~10 mmol/mol. Redox-sensitive trace elements (e.g. U; (Romaniello et al., 2013) and I/Ca; (Lu et al., 2010)) will have the added complication of sensitivity to the oxidation state of the diagenetic fluid. Pore-fluid profiles at Sites 1003 and 1007 (Eberli et al., 1997b) as well as fluids in reef and platform interiors (Tribble et al., 1992; Tribble, 1993; Falter and Sansone, 2000) suggest that reducing conditions associated with the oxidation of organic matter and other reduced species (e.g. H_2S) prevail even when there is significant fluid flow bringing oxidized bottom-water into the sediment-pore fluid system. As a result, while reducing conditions and preferential addition of U and loss of IO_3^- are expected for carbonate diagenesis under both sediment-buffered and fluid-buffered conditions, our results indicate that it may be particularly severe under fluid-buffered conditions. Observations of elevated $\delta^{44}Ca$ values and U/Mg +Ca ratios in bulk sediments from the Bahamas are consistent with this prediction (Fig. 9), though we note that the noise of the data suggests that the relationship between major element chemistry and U in the bulk sediment is complex.

Second, the isotopic fractionation factors and partition coefficients used in many of the proxies depend on mineralogy. For example, $\delta^{7}Li$ values in inorganic aragonite are ~8–10‰ depleted compared to calcite precipitated under similar conditions (Marriott et al., 2004). Similarly, the abundance of carbonate-associated sulfate (CAS) in inorganic calcite precipitated from seawater is typically 10,000's of ppm whereas it is substantially lower (1000's of ppm) in inorganic aragonite (Busenberg and Plummer, 1985). U partitioning also depends on mineralogy, though in this case U in inorganic aragonite is high (~2 ppm) and low in inorganic calcite (<0.4 ppm; (Chen et al., 2016)). Although this will not affect the $\delta^{34}S$ of CAS or $\delta^{238/235}U$ values directly, it could, through variations in mineralogy and styles of early marine diagenesis (of the kind seen in Site 1003, 1007, and Clino), produce stratigraphic variability in CAS or U contents. As minerals with low CAS (aragonite) or U (calcite) will be significantly more susceptible to contamination by later burial diagene-

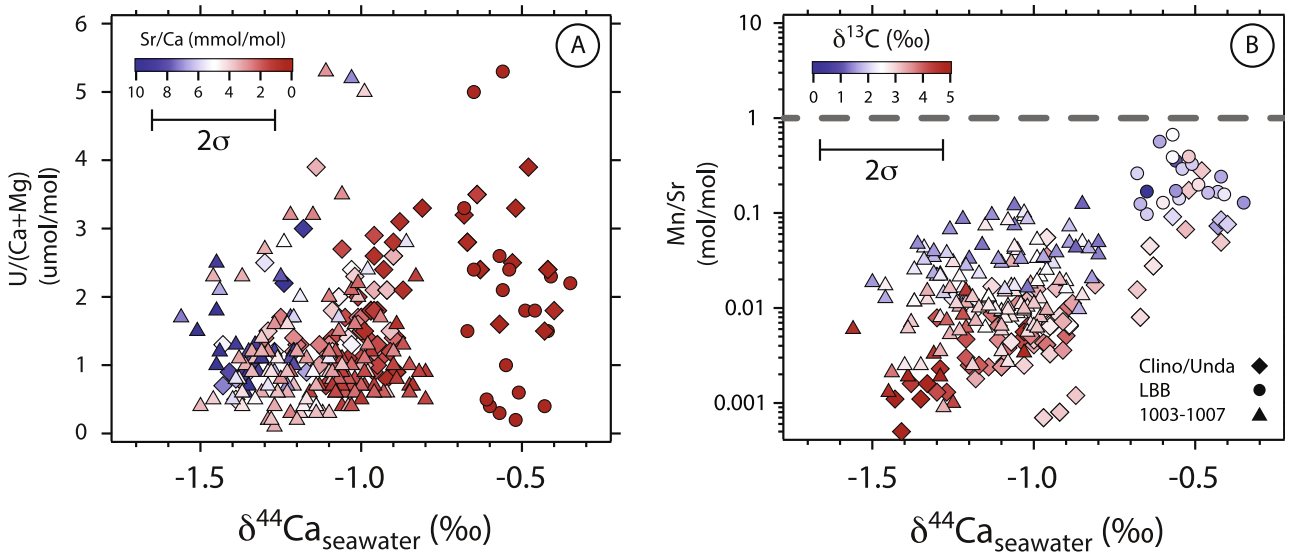

Fig. 9. Co-variation between bulk sediment $\delta^{44}Ca$ values and trace elements (U/(Ca+Mg) and Mn/Sr ratios) at the Bahamas sites. (A) Samples are colored by measured Sr/Ca ratio. Diagenetic U enrichment is seen in samples that have experienced both fluid-buffered (high $\delta^{44}Ca$ values) and sediment-buffered (low $\delta^{44}Ca$ values) early marine diagenesis, but it appears most severe in sediments diagenetically altered under fluid-buffered conditions. (B) Samples are colored by measured $\delta^{13}C$ value. Overall Mn/Sr ratios are positively correlated to bulk sediment $\delta^{44}Ca$ values with higher Mn/Sr ratios indicating more extensive diagenetic alteration. However, all samples fall well below the threshold Mn/Sr value of 1 (dashed grey line) often used in studies of ancient carbonate sediments. (For interpretation of the references to color in this figure legend, the reader is referred to the web version of this article.)

sis, authigenic mineral formation, partial dissolution of other phases (Marenco et al., 2008), and stratigraphic variability in CAS and U contents may lead to stratigraphic variations in $\delta^{34}S$ and $\delta^{238/235}U$ values that are unrelated to global seawater chemistry.

Third, to the extent that negative excursions in bulk sediment $\delta^{44}Ca$ values indicate an increase in the transport and sedimentation of shallow-water aragonite (above and beyond changes in fluid-buffered and sediment-buffered diagenesis) we expect that geochemical signals associated with mixing between shallow-water and pelagic environments may give rise to stratigraphic profiles and co-variation between geochemical proxies that are not related to changes in the global carbon cycle or seawater chemistry. Prior to expansion of pelagic calcification in the Mid-Mesozoic most carbonate sediment is thought to have precipitated in shallow-water platform, ramp, and marginal marine environments. However, other components of the bulk sediment, in particular sinking organic matter and early diagenetic phases (e.g. pyrite) likely had both shallow-water and more pelagic sources with distinct geochemical characteristics (i.e. $\delta^{13}C_{org}$ and $\delta^{34}S_{pyrite}$ values). Dilution of these pelagic signals by increased delivery of shallow-water carbonate sediment (with bank-top $\delta^{13}C_{org}$, $\delta^{13}C_{carb}$, $\delta^{34}S_{CAS}$, and $\delta^{34}S_{pyrite}$ values) may yield co-variation in paired $\delta^{13}C_{org}$ and $\delta^{13}C_{carb}$ values (Oehlert et al., 2012; Oehlert and Swart, 2014) or $\delta^{34}S_{pyrite}$ and $\delta^{34}S_{CAS}$ values that are also unrelated to changes in the global carbon and sulfur cycles.

5.5.3. Mn/Sr ratios as a proxy for diagenetic alteration in ancient carbonate sediments

Although originally developed to screen ancient carbonate sediments for $^{87}Sr/^{86}Sr$ analyses (Derry et al., 1992), Mn/Sr ratios are frequently used as an indicator of diagenetic alteration with a threshold of ~1–2 typically applied to exclude samples from further consideration. The foundation of this diagenetic indicator is that most subsurface (i.e. diagenetic) fluids are low in Sr and high in Mn (Brand and Veizer, 1980). As a result, recrystallization, neomorphism, or dolomitization in this fluid will tend to raise the Mn/Sr ratio of the carbonate sediment. Considered in this context, samples from this study show a positive correlation between Mn/Sr ratio and bulk sediment $\delta^{44}Ca$ values with higher Mn/Sr ratios associated with more positive $\delta^{44}Ca$ values (Fig. 8B). However, for all the variability in sediment Mn/Sr ratios even the most altered bulk carbonates have Mn/Sr ratios <1. In other words, the use of a threshold Mn/Sr ratio of 1 would suggest that diagenetic alteration in the Bahamas sites has been relatively minor in spite of multiple independent lines of geochemical evidence that indicate otherwise. Although the correlation between bulk sediment $\delta^{44}Ca$ values and Mn/Sr ratios (Fig. 9) suggests that this proxy may provide some information on the relative extent of diagenetic alteration, we strongly urge against any use of threshold values of Mn/Sr ratios when trying to determine the potential for diagenetic alteration in ancient carbonate sediments.

5.5.4. Implications for modern $\delta^{44}Ca_{seawater}$ mass balance and shelf-basin partitioning of global carbonate sediments

Fantle and Tipper (2014) compiled a large database of published Ca isotope values taken from the literature and applied a statistical evaluation of the data to deduce average δ^{44}Ca values for the major Ca sources and sinks in the Earth's modern exogenic Ca cycle. They concluded from this analysis the δ^{44}Ca value of bulk silicate Earth and global rivers is ~0.3‰ enriched in ^{44}Ca relative to deep-sea carbonate sediments. Rivers are the principle source of Ca to seawater and carbonate sediments are the overwhelming sink. The imbalance of 0.3‰ could represent non-steady state conditions, however, an equally plausible explanation is that there exists a significantly undersampled carbonate sink enriched in ^{44}Ca. Results from this study and previous work by Fantle & Higgins (Fantle and Higgins, 2014) and Blättler et al. (Blättler et al., 2015) suggest that this missing sink could be a combination of shallow-water fluid-buffered diagenetic and authigenic carbonates. Shallow-water carbonate sediments are underrepresented in the Fantle and Tipper (2014) compilation and yet represent a large fraction of the global sedimentary carbonate sink. The average δ^{44}Ca value of samples from platform interiors and margins is −0.90‰ (Clino, Unda, and LBB; $N = 108$) whereas those from only the platform interior average −0.53‰ (Unda and LBB; $N = 22$). These δ^{44}Ca values are 0.4–0.7‰ enriched in ^{44}Ca relative to the average deep-sea carbonate sink (−1.25‰) and 0.1–0.4‰ enriched relative to bulk silicate Earth (−0.98‰; (Fantle and Tipper, 2014)). Assuming the modern ocean is near steady-state with respect to Ca isotopes and an average δ^{44}Ca value of −0.75‰ for diagenetically stabilized shallow-water platform carbonates we estimate a ~50/50 partitioning of carbonate burial in shallow-water and deep-sea sediments. This geochemical estimate of present-day shelf to deep partitioning of global carbonate burial is similar to but entirely independent of estimates based on sediment seismic surveys, drill cores, and measurements of modern accumulation rates (Milliman and Droxler, 1996).

Our results also provide additional evidence that the δ^{44}Ca of seawater on geologic timescales may not be governed by changes in the mineralogy of marine carbonate precipitates (the 'aragonite seas' and 'calcite seas' of Sandberg (1983)). Although sediment-buffered neomorphosed aragonite (low δ^{44}Ca values) can be preserved on continental slopes (e.g. Sites 1003 and 1007), any Ca isotopic signal of aragonite in bulk sediment on the platform margin and interior (Clina, Unda, and LBB) has been dramatically shifted towards higher δ^{44}Ca values; average δ^{44}Ca values are more positive than bulk silicate Earth or exactly the opposite of that predicted for an 'aragonite sea' (Farkas et al., 2007). Given the central role of fluid flow in the diagenesis of carbonate sediments on platform tops and margins and its effect on the δ^{44}Ca value of the shallow-water carbonate sink we speculate that the δ^{44}Ca value of seawater may be controlled, in part, by changes in the volume of shallow-water carbonate sediments through time. Lower seawater δ^{44}Ca values would be expected during periods of abundant shallow-water carbonate sediments (and associated fluid-buffered diagenesis) whereas higher seawater δ^{44}Ca values would be expected when there is a significant deep-sea carbonate sink (where diagenesis is predominantly sediment-buffered). In this regard the growth of a large deep-sea carbonate sink since the Mesozoic (at the expense of carbonate sedimentation in shallow-water environments (Opdyke and Wilkinson, 1988)) should be associated with an increase in the δ^{44}Ca of seawater, consistent in sign with observations from fossil corals (Gothmann et al., 2016), fossil carbonates and barite (Farkas et al., 2007; Griffith et al., 2008; Blättler et al., 2012) and minimum δ^{44}Ca values of seawater-derived sedimentary $CaSO_4$ (Blättler and Higgins, 2014).

5.5.5. Implications for modern global $\delta^{26}Mg_{seawater}$ mass balance and dolomitization

Sedimentary dolomite is believed to play an outsized role in the regulation of seawater Mg/Ca ratios on geologic timescales (Wilkinson and Algeo, 1989; Holland and Zimmerman, 2000). The Mg isotope data offer an excellent opportunity to study this enigmatic process because its formation is associated with Mg isotope fractionation (Young and Galy, 2004; Higgins and Schrag, 2010; Li et al., 2015). This isotopic leverage permits, assuming the modern system is close to steady-state, an estimate of the relative importance of dolomite as a global Mg sink. Using this approach, Tipper et al. (2006) arrived at an estimate that at least ~10% of the Mg sink in the modern ocean is associated with the formation of sedimentary dolomite. As discussed in Section 4.4 a critical variable in this estimate is the average Mg isotope fractionation factor associated with the dolomite sink. Our results provide additional support for $\alpha^{26/24}_{dolomite} = 0.9980$, the value used by Tipper et al. (2006). However, this is likely an upper estimate as net fractionation of Mg isotopes will be smaller in sediment-buffered dolomites. For example, the dolomites from the Bahamas average -2.79 ± 0.17‰ (2σ; $N = 80$) whereas the authigenic dolomites from the Monterey Fm. average -2.06 ± 1.13‰ (2σ; $N = 45$).

6. CONCLUSIONS

Shallow-water carbonate sediments are one of the most extensive and well-studied records of the chemistry and temperature of ancient oceans (Veizer and Hoefs, 1976; Veizer et al., 1999; Kasting et al., 2006). One of the major limitations in the utilization of this archive is the potential for changes in the chemical composition of the sediments at any time after they were initially precipitated. Using a large data set of Ca and Mg isotope measurements in Neogene shallow-water carbonate sediments and associated porefluids from the platform to the slope in the Bahamas we have shown that stratigraphic variability in these isotopic systems is due to variations in both mineralogy and style of diagenetic alteration (fluid-buffered vs. sediment-buffered). This interpretation is rather counterintuitive given that these elements, and Ca in particular, are major components of the carbonate sediment and should be relatively robust – almost as robust as C – to diagenetic alteration. However, the large magnitude of the stratigraphic

variability in bulk sediment $\delta^{44}Ca$ values – up to 1‰ – cannot be explained by mixing of sediment from different sources or secular variability in the $\delta^{44}Ca$ value of seawater. Rather, the variability in bulk sediment $\delta^{44}Ca$ values both within and between sites – in particular the presence of bulk sediment $\delta^{44}Ca$ values that are significantly higher than modern bank-top sediments – appears to be the consequence of progressive recrystallization/neomorphism under fluid-buffered diagenetic conditions. This process implies globally significant mass fluxes of Ca between seawater and shallow marine pore-fluids, consistent with observations of active fluid flow and neomorphism/recrystallization within the upper 10's of meters of the sediment column from pore-fluid profiles of $[Cl^-]$, $[Ca^{2+}]$, and $\delta^{44}Ca$ values at some of the Bahamas sites. Modeled rates of recrystallization/neomorphism using the pore-fluid profiles favor rates that are both higher than those observed in the deep-sea and capable of re-setting bulk and trace element chemistry of the sediment on million-year timescales.

In contrast to the large stratigraphic variability observed in sediment $\delta^{44}Ca$ values, sediment $\delta^{26}Mg$ values exhibit much less variability – an apparent consequence of similar Mg isotope fractionation in high-Mg calcite and dolomite. Paired measurements of $\delta^{26}Mg$ and $\delta^{44}Ca$ values in dolomites exhibit co-variation that is consistent with dolomitization in the Bahamas occurring under both fluid-buffered and sediment-buffered conditions, with fluid-buffered conditions predominating. This approach provides a means for distinguishing between chemical signals in dolomite from the precursor carbonate vs. those from the dolomitizing fluid.

The observation that sediment $\delta^{44}Ca$ values in Neogene shallow-water carbonate sediments from the platform top, margin, and slope are largely controlled by mineralogy and the extent of fluid-buffered early marine diagenesis and that temporal variations in fluid-buffered diagenesis can generate stratigraphically coherent co-variation between many carbonate-bound geochemical proxies ($\delta^{13}C$, $\delta^{18}O$, Sr/Ca, etc.) has significant implications for the interpretation of both the major and trace element chemistry of shallow-water carbonate sediments in the geologic record. In particular, it suggests that stratigraphic co-variation between carbonate-bound geochemical proxies need not reflect changes in the global geochemical cycles of these elements but rather changes in the composition of bank-top waters and/or the extent of fluid-buffered vs. sediment-buffered early marine diagenesis. Thus, records of secular change and extreme variability in shallow-water carbonate sediments might be better interpreted as records of the effects of global environmental change and evolution on shallow-water carbonate-producing environments and not archives of global geochemical fluxes (e.g. the relative rates of organic carbon and carbonate burial from the $\delta^{13}C$ of $CaCO_3$).

Our data also provide new constraints on both Ca and Mg isotope mass balance in the modern ocean. The observation of carbonate sediments enriched in ^{44}Ca in shallow-water environments is contrary to the expectation of variations in the $\delta^{44}Ca$ of seawater due to changes in primary sediment mineralogy – i.e. 'calcite and aragonite' seas. In addition, a shallow-water carbonate sink that is characterized by $\delta^{44}Ca$ values that are higher than bulk silicate Earth can likely explain the observation that deep-sea carbonate sediments (the other major sink of Ca from seawater) are ~0.3‰ lower than bulk silicate Earth. Finally, estimates of Mg isotope fractionation during dolomitization from both bulk sediments and pore-fluids indicate that low-temperature dolomite should be ~2‰ depleted in ^{26}Mg compared to the precipitating fluid. This result supports the hypothesis that the formation of dolomite has a significant effect on the $\delta^{26}Mg$ of seawater but represents a relatively small sink of Mg in the modern ocean.

ACKNOWLEDGEMENTS

We would like to thank 2 anonymous reviewers Elizabeth Griffith for constructive comments that improved the manuscript. JAH acknowledges support from NSF grant no. IES1410317.

APPENDIX A. SUPPLEMENTARY MATERIAL

Supplementary data associated with this article can be found, in the online version, at https://doi.org/10.1016/j.gca.2017.09.046.

REFERENCES

Banner J. L. and Hanson G. N. (1990) Calculation of simultaneous isotopic and trace-element variations during water-rock interaction with applications to carbonate diagenesis. *Geochim. Cosmochim. Acta* **54**, 3123–3137.

Belanger N. and Holmden C. (2010) Influence of landscape on the apportionment of Ca nutrition in a Boreal Shield forest of Saskatchewan (Canada) using Sr-87/Sr-86 as a tracer. *Can. J. Soil Sci.* **90**, 267–288.

Berner R. A. (1966) Chemical diagenesis of some modern carbonate sediments. *Am. J. Sci.*, 1–13.

Blättler C. L., Henderson G. M. and Jenkyns H. C. (2012) Explaining the Phanerozoic Ca isotope history of seawater. *Geology* **40**, 843–846.

Blättler C. L. and Higgins J. A. (2014) Calcium isotopes in evaporites record variations in Phanerozoic seawater SO4 and Ca. *Geology* **42**, 711–714.

Blättler C. L., Miller N. R. and Higgins J. A. (2015) Mg and Ca isotope signatures of authigenic dolomite in siliceous deep-sea sediments. *Earth Planet. Sci. Lett.* **419**, 32–42.

Boss S. K. and Wilkinson B. H. (1991) Planktogenic eustatic control on cratonic oceanic carbonate accumulation. *J. Geol.* **99**, 497–513.

Brand U. and Veizer J. (1980) Chemical diagenesis of a multicomponent carbonate system. 1) trace elements. *J. Sediment. Petrol.* **50**, 1219–1236.

Budd D. A. (1997) Cenozoic dolomites of carbonate islands: their attributes and origin. *Earth Sci. Rev.* **42**, 1–47.

Busenberg E. and Plummer L. N. (1985) Kinteic and thermodynamic factors controlling the distibution of SO4(2-) and Na+ in calcites and selected aragonites. *Geochim. Cosmochim. Acta* **49**, 713–725.

Caspard E., Rudkiewicz J. L., Eberli G. P., Brosse E. and Renard M. (2004) Massive dolomitization of a Messinian reef in the Great Bahama Bank: a numerical modelling evaluation of Kohout geothermal convection. *Geofluids* **4**, 40–60.

Chen X. M., Romaniello S. J., Herrmann A. D., Wasylenki L. E. and Anbar A. D. (2016) Uranium isotope fractionation during coprecipitation with aragonite and calcite. *Geochim. Cosmochim. Acta* **188**, 189–207.

Compton J. S. and Siever R. (1986) Diffusion and mass balance of Mg during early dolomite formation, Monterey Formation. *Geochim. Cosmochim. Acta* **50**, 125–135.

DePaolo D. J. (2011) Surface kinetic model for isotopic and trace element fractionation during precipitation of calcite from aqueous solutions. *Geochim. Cosmochim. Acta* **75**, 1039–1056.

Derry L. A. (2010) A burial diagenesis origin for the Ediacaran Shuram-Wonoka carbon isotope anomaly. *Earth Planet. Sci. Lett.* **294**, 152–162.

Derry L. A., Kaufman A. J. and Jacobsen S. B. (1992) Sedimentary cycling and environmental change in the Late Proterozoic - evidence from stable and ratiogenic isotopes. *Geochim. Cosmochim. Acta* **56**, 1317–1329.

Droxler A. W., Schlager W. and Whallon C. C. (1983) Quaternary aragonite cycles and oxygen-isotope records in Bahamanian carbonate ooze. *Geology* **11**, 235–239.

Eberli G., Swart P. K., McNeill D. F., Kenter J. A. M., Anselmetti F. S., Melim L. A. and Ginsburg R. N. (1997a) Leg 166 - Bahamas Drilling Project. Initial Reports of the Ocean Drilling Program.

Eberli G. P. and Ginsburg R. N. (1987) Segmentation and coalescence of Cenozoic carbonate platforms, Northwestern Great Bahama Bank. *Geology* **15**, 75–79.

Eberli G. P., Swart P. K. and Malone M. J. (1997b) Leg 166, Proceedings of the Ocean Drilling Program, Initial Reports. Ocean Drilling Program, College Station, TX.

Edgar K. M., Anagnostou E., Pearson P. N. and Foster G. L. (2015) Assessing the impact of diagenesis on d11B, d13C, d18O, Sr/Ca and B/Ca values in fossil planktic foraminiferal calcite. *Geochim. Cosmochim. Acta* **166**, 189–209.

Falter J. L. and Sansone F. J. (2000) Hydraulic control of pore water geochemistry within the oxic-suboxic zone of a permeable sediment. *Limnol. Oceanogr.* **45**, 550–557.

Fantle M. S. and DePaolo D. J. (2007) Ca isotopes in carbonate sediment and pore fluid from ODP Site 807A: the Ca2+(aq)-calcite equilibrium fractionation factor and calcite recrystallization rates in Pleistocene sediments. *Geochim. Cosmochim. Acta* **71**, 2524–2546.

Fantle M. S. and Higgins J. (2014) The effects of diagenesis and dolomitization on Ca and Mg isotopes in marine platform carbonates: implications for the geochemical cycles of Ca and Mg. *Geochim. Cosmochim. Acta* **142**, 458–481.

Fantle M. S. and Tipper E. T. (2014) Calcium isotopes in the global biogeochemical Ca cycle: implications for development of a Ca isotope proxy. *Earth Sci. Rev.* **129**, 148–177.

Farkas J., Bohm F., Wallmann K., Blenkinsop J., Eisenhauer A., Vangeldern R., Munnecke A., Voigt S. and Veizer J. (2007) Calcium isotope record of Phanerozoic oceans: implications for chemical evolution of seawater and its causative mechanisms. *Geochim. Cosmochim. Acta* **71**, 5117–5134.

Feary D. A., Hine A. C. and Malone M. J. (2000) Leg 182. Proceedings of the Ocean Drilling Program, Initial Reports.

Garcia-Fresca B., Lucia F. J., Sharp J. M. and Kerans C. (2012) Outcrop-constrained hydrogeological simulations of brine reflux and early dolomitization of the Permian San Andres Formation. *Aapg Bull.* **96**, 1757–1781.

Geske A., Goldstein R. H., Mavromatis V., Richter D. K., Buhl D., Kluge T., John C. M. and Immenhauser A. (2015a) The magnesium isotope (delta Mg-26) signature of dolomites. *Geochim. Cosmochim. Acta* **149**, 131–151.

Geske A., Lokier S., Dietzel M., Richter D. K., Buhl D. and Immenhauser A. (2015b) Magnesium isotope composition of sabkha porewater and related (Sub-) Recent stoichiometric dolomites, Abu Dhabi (UAE). *Chem. Geol.* **393–394**, 112–124.

Ginsburg R. N. (1957) Early diagenesis and lithification of shallow-water carbonate sediments in south Florida. *Spec. Publ. Soc. Econ. Paleontol. Mineral.* **5**, 80–100.

Ginsburg R. N. (2001) The Bahamas drilling project: background and acquisition of the cores and logs. In: Ginsburg R. N. (Ed.), Subsurface Geology of a Prograding Carbonate Platform Margin, Great Bahama Bank: Results from the Bahama Drilling Project ed Ginsburg RN (Society for Sedimentary Geology), pp. 3–16.

Gothmann A. M., Bender M. L., Blättler C. L., Swart P. K., Giri S. J., Adkins J. F., Stolarski J. and Higgins J. A. (2016) Calcium isotopes in scleractinian fossil corals since the Mesozoic: implications for vital effects and biomineralization through time. *Earth Planet. Sci. Lett.* **444**, 205–214.

Griffith E. M., Paytan A., Caldeira K., Bullen T. D. and Thomas E. (2008) A dynamic marine calcium cycle during the past 28 million years. *Science* **322**, 1671–1674.

Gussone N., Bohm F., Eisenhauer A., Dietzel M., Heuser A., Teichert B. M. A., Reitner J., Worheide G. and Dullo W. C. (2005) Calcium isotope fractionation in calcite and aragonite. *Geochim. Cosmochim. Acta* **69**, 4485–4494.

Hardie L. A. (1987) Dolomitization - a critical view of some current views. *J. Sediment. Petrol.* **57**, 166–183.

Henderson G. M., Slowey N. C. and Haddad G. A. (1999) Fluid flow through carbonate platforms: constraints from U-234/U-238 and Cl- in Bahamas pore-waters. *Earth Planet. Sci. Lett.* **169**, 99–111.

Higgins J. A. and Schrag D. P. (2010) Constraining magnesium cycling in marine sediments using magnesium isotopes. *Geochim. Cosmochim. Acta* **74**, 5039–5053.

Higgins J. A. and Schrag D. P. (2012) Records of Neogene seawater chemistry and diagenesis in deep-sea carbonate sediments and pore fluids. *Earth Planet. Sci. Lett.* **357**, 386–396.

Higgins J. A. and Schrag D. P. (2015) The Mg isotopic composition of Cenozoic seawater- evidence for a link between Mg-clays, seawater Mg/Ca, and climate. *Earth Planet. Sci. Lett.* **416**, 73–81.

Holland H. D. and Zimmerman H. (2000) The dolomite problem revisited. *Int. Geol. Rev.* **42**, 481–490.

Holmden C. (2005) Measurement of d44Ca using a43Ca-42Ca double-spike TIMS technique. Saskatchewan Industry and Resources Miscellaneous Report 2005, CD-ROM, Paper A-4, 7p.

Holmden C. (2009) Ca isotope study of Ordovician dolomite, limestone, and anhydrite in the Williston Basin: implications for subsurface dolomitization and local Ca cycling. *Chem. Geol.* **268**, 180–188.

Holmden C., Creaser R. A., Muehlenbachs K., Leslie S. A. and Bergstrom S. M. (1998) Isotopic evidence for geochemical decoupling between ancient epeiric seas and bordering oceans: implications for secular curves. *Geology* **26**, 567–570.

Holmden C., Papanastassiou D. A., Blanchon P. and Evans S. (2012) D44/40Ca variability in shallow water carbonates and the impact of submarine groundwater discharge on Ca-cycling in marine environments. *Geochim. Cosmochim. Acta* **83**, 179–194.

Horita J. (2014) Oxygen and carbon isotope fractionation in the system dolomite-water-CO_2 to elevated temperatures. *Geochim. Cosmochim. Acta* **129**, 111–124.

Husson J. M., Higgins J. A., Maloof A. C. and Schoene B. (2015) Ca and Mg isotope constraints on the origin of Earth's deepest delta C-13 excursion. *Geochim. Cosmochim. Acta* **160**, 243–266.

Immenhauser A., Della Porta G., Kenter J. A. M. and Bahamonde J. R. (2003) An alternative model for positive shifts in shallow-

marine carbonate delta C-13 and delta O-18. *Sedimentology* **50**, 953–959.

Jacobson A. D. and Holmden C. (2008) Delta(44)Ca evolution in a carbonate aquifer and its bearing on the equilibrium isotope fractionation factor for calcite. *Earth Planet. Sci. Lett.* **270**, 349–353.

Jones G. D., Whitaker F. F., Smart P. L. and Sanford W. E. (2004) Numerical analysis of seawater circulation in carbonate platforms: II. The dynamic interaction between geothermal and brine reflux circulation. *Am. J. Sci.* **304**, 250–284.

Kasting J. F., Howard M. T., Wallmann K., Veizer J., Shields G. and Jaffres J. (2006) Paleoclimates, ocean depth, and the oxygen isotopic composition of seawater. *Earth Planet. Sci. Lett.* **252**, 82–93.

Kaufman J. (1994) Numerical models of fluid-flow in carbonate platforms - implications for dolomitization. *J. Sediment. Res. Section a-Sediment. Petrol. Processes* **64**, 128–139.

Kenter J. A. M., Ginsburg R. N. and Troelstra S. R. (2001) Sea-level driven sedimentation patterns on the slope and margin. In *Subsurface Geology of a Prograding Carbonate Platform Margin* (ed. R. N. Ginsburg). Results of the Bahama Drilling Project. Society for Sedimentary Geology, Great Bahama Bank, pp. 61–101.

Knauth L. P. and Kennedy M. J. (2009) The late Precambrian greening of the Earth. *Nature* **460**, 728–732.

Kozdon R., Kelly D. C., Kita N. T., Fournelle J. H. and Valley J. W. (2011) Planktonic foraminiferal oxygen isotope analysis by ion microprobe technique suggests warm tropical sea surface temperatures during the Early Paleogene. *Paleoceanography* **26**.

Kramer P. A., Swart P. K., De Carlo E. H. and Schovsbo N. H. (2000) Overview of Leg 166 interstitial fluid and sediment geochemistry, Sites 1003–1007 (Bahamas Transect). In Proceedings of the Ocean Drilling Program - Scientific Results (eds. P.K. Swart, G.P. Eberli, M.J. Malone). College Station, Ocean Drilling Program. pp. 179–198.

Land L. S. (1998) Failure to precipitate dolomite at 25 degrees C from dilute solution despite 1000-fold oversaturation after 32 years. *Aquat. Geochem.* **4**, 361–368.

Lehn G. O., Jacobson A. D. and Holmden C. (2013) Precise analysis of Ca isotope ratios (delta(44/40)ca) using an optimized Ca-43-Ca-42 double-spike MC-TIMS method. *Int. J. Mass Spectrom.* **351**, 69–75.

Li W. Q., Beard B. L., Li C. X., Xu H. F. and Johnson C. M. (2015) Experimental calibration of Mg isotope fractionation between dolomite and aqueous solution and its geological implications. *Geochim. Cosmochim. Acta* **157**, 164–181.

Li W. Q., Chakraborty S., Beard B. L., Romanek C. S. and Johnson C. M. (2012) Magnesium isotope fractionation during precipitation of inorganic calcite under laboratory conditions. *Earth Planet. Sci. Lett.* **333**, 304–316.

Lu Z. L., Jenkyns H. C. and Rickaby R. E. M. (2010) Iodine to calcium ratios in marine carbonate as a paleo-redox proxy during oceanic anoxic events. *Geology* **38**, 1107–1110.

Marenco P. J., Corsetti F. A., Hammond D. E., Kaufman A. J. and Bottjer D. J. (2008) Oxidation of pyrite during extraction of carbonate associated sulfate. *Chem. Geol.* **247**, 124–132.

Marriott C. S., Henderson G. M., Belshaw N. S. and Tudhope A. W. (2004) Temperature dependence of d^7Li, d^{44}Ca and Li/Ca during growth of calcium carbonate. *Earth Planet. Sci. Lett.* **222**, 615–624.

Marshall J. D. (1992) Climatic and oceanographic isotopic signals from the carbonate rock record and their preservation. *Geol. Mag.* **129**, 143–160.

Melim L. A., Swart P. K. and Eberli G. P. (2004) Mixing-zone diagenesis in the subsurface of Florida and The Bahamas. *J. Sediment. Res.* **74**, 904–913.

Melim L. A., Swart P. K. and Maliva R. G. (2001) Meteoric and marine-burial diagenesis in the subsurface of the Great Bahama Bank. In: Subsurface geology of a prograding carbonate platform margin, Great Bahama Bank: results of the Bahama Drilling Project (eds. R.N. Ginsburg). Society for Sedimentary Geology. pp. 137–163.

Milliman J. D. and Droxler A. W. (1996) Neritic and pelagic carbonate sedimentation in the marine environment: ignorance is not bliss. *Geol. Rundsch.* **85**, 496–504.

Morse J. and Mackenzie F. T. (1990) *Geochemistry of Sedimentary Carbonates*. Elsevier, Amsterdam.

Muehlenbachs K. and Clayton R. N. (1976) Oxygen isotope composition of oceanic-crust and its bearing on seawater. *J. Geophys. Res.* **81**, 4365–4369.

Murray S. and Swart P. K. (2017) Evaluating formation fluid models and calibrations using clumped isotope paleothermometry on bahamian dolomites. *Geochim. Cosmchim. Acta* **2061**, 73–93.

Nielsen L. C., De Yoreo J. J. and DePaolo D. J. (2013) General model for calcite growth kinetics in the presence of impurity ions. *Geochim. Cosmochim. Acta* **115**, 100–114.

Oehlert A. M., Lamb-Wozniak K. A., Devlin Q. B., Mackenzie G. J., Reijmer J. J. G. and Swart P. K. (2012) The stable carbon isotopic composition of organic material in platform derived sediments: implications for reconstructing the global carbon cycle. *Sedimentology* **59**, 319–335.

Oehlert A. M. and Swart P. K. (2014) Interpreting carbonate and organic carbon isotope covariance in the sedimentary record. *Nat. Commun.* **5**.

Opdyke B. N. and Wilkinson B. H. (1988) Surface area control of shallow cratonic to deep marine carbonate accumulation. *Paleoceanography* **3**, 685–703.

Patterson W. P. and Walter L. M. (1994) Syndepositional diagenesis of modern platform carbonates - evidence from isotopic and minor element data. *Geology* **22**, 127–130.

Rennie V. C. F. and Turchyn A. V. (2014) The preservation of delta S-34(SO4) and delta O-18(SO4) in carbonate-associated sulfate during marine diagenesis: a 25 Myr test case using marine sediments. *Earth Planet. Sci. Lett.* **395**, 13–23.

Richter F. M. and DePaolo D. J. (1987) Numerical models for diagenesis and the Neogene Sr isotopic evolution of seawater from DSDP Site 590B. *Earth Planet. Sci. Lett.* **83**, 27–38.

Ridgwell A. (2005) A Mid Mesozoic revolution in the regulation of ocean chemistry. *Mar. Geol.* **217**, 339–357.

Riechelmann S., Mavromatis V., Buhl D., Dietzel M., Eisenhauer A. and Immenhauser A. (2016) Impact of diagenetic alteration on brachiopod shell magnesium isotope (delta Mg-26) signatures: experimental versus field data. *Chem. Geol.* **440**, 191–206.

Romaniello S. J., Herrmann A. D. and Anbar A. D. (2013) Uranium concentrations and U-238/U-235 isotope ratios in modern carbonates from the Bahamas: assessing a novel paleoredox proxy. *Chem. Geol.* **362**, 305–316.

Rosenthal Y., Field M. P. and Sherrell R. M. (1999) Precise determination of element/calcium ratios in calcareous samples using sector field inductively coupled plasma mass spectrometry. *Anal. Chem.* **71**, 3248–3253.

Rudge J. F., Reynolds B. C. and Bourdon B. (2009) The double spike toolbox. *Chem. Geol.* **265**, 420–431.

Sandberg P. A. (1983) An oscillating trend in Phanerozoic non-skeletal carbonate mineralogy. *Nature* **305**, 19–22.

Sass E. and Katz A. (1982) The origin of platform dolomites - new evidence. *Am. J. Sci.* **282**, 1184–1213.

Saulnier S., Rollion-Bard C., Vigier N. and Chaussidon M. (2012) Mg isotope fractionation during calcite precipitation: an experimental study. *Geochim. Cosmochim. Acta* **91**, 75–91.

Sayles F. L. and Manheim F. T. (1975) Interstitial solutions and diagenesis in deeply buried marine sediments: results from the Deep Sea Drilling Project. *Geochim. Cosmochim. Acta* **39**, 103–127.

Schmitt A.-D., Gangioff S., Cobert F., Lemarchand D., Stille P. and Chabaux F. (2009) High performance automated ion chromatography separation for Ca isotope measurements in geological and biological samples. *J. Anal. Atom. Spectrom.* **24**, 1089–1097.

Schrag D. P., DePaolo D. J. and Richter F. M. (1995) Reconstructing past sea-surface temperatures - correcting for diagenesis of bulk marine carbonate. *Geochim. Cosmochim. Acta* **59**, 2265–2278.

Schrag D. P., Higgins J. A., Macdonald F. A. and Johnston D. T. (2013) Authigenic carbonate and the history of the global carbon cycle. *Science* **339**, 540–543.

Swart P. (2000) The oxygen isotopic composition of interstitial waters: evidence for fluid flow and recrystallization in the margin of the Great Bahama Bank. Initial reports of the ocean drilling porgram. *Sci. Results* **166**, 91–98.

Swart P. K. (2008) Global synchronous changes in the carbon isotopic composition of carbonate sediments unrelated to changes in the global carbon cycle. *Proc. Natl. Acad. Sci. USA* **105**, 13741–13745.

Swart P. K. (2015) The geochemistry of carbonate diagenesis: the past, present and future. *Sedimentology* **62**, 1233–1304.

Swart P. K. and Eberli G. P. (2005) The nature of the d13C of periplatform sediments: Implications for stratigraphy and the global carbon cycle. *Sed. Geol.* **175**, 115–129.

Swart P. K. and Melim L. A. (2000) The origin of dolomites in tertiary sediments from the margin of Great Bahama Bank. *J. Sediment. Res.* **70**, 738–748.

Swart P. K., Reijmer J. J. G. and Otto R. (2009) A re-evaluation of facies on Great Bahama Bank II: Variations in the d13C, d18O and mineralogy of surface sediments. Perspectives in Carbonate Geology: a Tribute to the Career of Robert Nathan Ginsburg 41, 47–59.

Swart P. K., Wortmann U. G., Mitterer R. M., Malone M. J., Smart P. L., Feary D. A. and Hine A. C. (2000) Hydrogen sulfide-rich hydrates and saline fluids in the continental margin of South Australia. *Geology* **28**, 1039–1042.

Tang J., Dietzel M., Bohm A., Kohler P. and Eisenhauer A. (2008) Sr^{2+}/Ca^{2+} and $^{44}Ca/^{40}Ca$ fractioning during inorganic calcite formation: II. Ca isotopes. *Geochimica et Cosmochimica Acta* **72**, 3733–3745.

Tipper E. T., Galy A., Gaillardet J., Bickle M. J., Elderfield H. and Carder E. A. (2006) The magnesium isotope budget of the modem ocean: constraints from riverine magnesium isotope ratios. *Earth Planet. Sci. Lett.* **250**, 241–253.

Tribble G. W. (1993) Organic-matter oxidation and aragonite diagenesis in a coral-reef. *J. Sediment. Petrol.* **63**, 523–527.

Tribble G. W., Sansone F. J., Buddemeier R. W. and Li Y. H. (1992) Hydraulic exchange between a coral-reef and surface sea-water. *Geol. Soc. Am. Bull.* **104**, 1280–1291.

Turchyn A. V. and DePaolo D. J. (2011) Calcium isotope evidence for suppression of carbonate dissolution in carbonate-bearing organic-rich sediments. *Geochim. Cosmochim. Acta* **75**, 7081–7098.

Vahrenkamp V. C., Swart P. K. and Ruiz J. (1988) Constraints and interpretation of 87Sr/86Sr ratios in Cenozoic dolomites. *Geophys. Res. Lett.* **15**, 385–388.

Vahrenkamp V. C., Swart P. K. and Ruiz J. (1991a) Episodic dolomitization of Late Cenozoic carbonates in the Bahamas - evidence from strontium isotopes. *J. Sediment. Petrol.* **61**, 1002–1014.

Vahrenkamp V. C., Swart P. K. and Ruiz J. (1991b) Episodic dolomitization of late Cenozoic carbonates in the Bahamas - evidence from strontrium isotopes. *J. Sediment. Petrol.* **61**, 1002–1014.

Veizer J., Ala D., Azmy K., Bruckschen P., Buhl D., Bruhn F., Carden G. A. F., Diener A., Ebneth S., Godderis Y., Jasper T., Korte C., Pawellek F., Podlaha O. G. and Strauss H. (1999) 87Sr/86Sr, d13C and d18O evolution of Phanerozoic seawater. *Chem. Geol.* **161**, 59–88.

Veizer J. and Hoefs J. (1976) Nature of O18/O16 and C13/C12 secular trends in sedimentary carbonate rocks. *Geochim. Cosmochim. Acta* **40**, 1387–1395.

Walter L. M., Bischof S. A., Patterson W. P. and Lyons T. W. (1993) Dissolution and recrystallization in modern shelf carbonates - evidence from pore-water and solid-phase chemistry. *Philos. Trans. Roy. Soc. Lond. Ser. A – Math. Phys. Eng. Sci.* **344**, 27–36.

Wang Z., Hu P., Gaetani G. A., Liu C., Liu C., Saenger C., Cohen A. L. and Hart S. R. (2013) Experimental calibration of Mg isotope fractionation between aragonite and seawater. *Geochim. Cosmochim. Acta* **102**, 113–123.

Wilkinson B. H. and Algeo T. J. (1989) Sedimentary carbonate record of calcium and magnesium cycling. *Am. J. Sci.* **289**, 1158–1194.

Wombacher F., Eisenhauer A., Böhm F., Gussone N., Regenberg M., Dullo W. C. and Ruggeberg A. (2011) Magnesium stable isotope fractionation in marine biogenic calcite and aragonite. *Geochim. Cosmochim. Acta* **75**, 5797–5818.

Young E. D. and Galy A. (2004) The isotope geochemistry and cosmochemistry of magnesium. *Geochem. Non-Traditional Stable Isotopes* **55**, 197–230.

Associate editor: Fang-Zhen Teng